References

Adachi O, Ano Y, Toyama H & Matsushita K (2007) Biooxidation with PQQ- and FAD-dependent dehydrogenases. *Modern Biooxidation, Enzymes, Reactions and Applications* (Schmid RD & Urlacher VB, eds), pp. 1–41. Wiley-VCH, Weinheim.

Ameyama M, Matsushita K, Shinagawa E & Adachi O (1987) Sugar-oxidizing respiratory chain of *Gluconobacter suboxydans*. Evidence for a branched respiratory chain and characterization of respiratory chain-linked cytochromes. *Agr Biol Chem* **51**: 2943–2950.

Biagini GA, Viriyavejakul P, O'Neill PM, Bray PG & Ward SA (2006) Functional characterization and target validation of alternative Complex I of *Plasmodium falciparum* mitochondria. *Antimicrob Agents Ch* **50**: 1841–1851.

Björklöf K, Zickermann V & Finel M (2000) Purifiction of the 45 kDa, membrane bound NADH dehydrogenase of *Escherichia coli* (NDH-2) and analysis of its interaction with ubiquinone analogs. *FEBS Lett* **467**: 105–110.

Deppenmeier U, Hoffmeister M & Prust C (2002) Biochemistry and biotechnological applications of *Gluconobacter* strains. *Appl Microbiol Biot* **60**: 233–242.

De Vries S & Grivell LA (1988) Purification and characterization of a rotenone-insensitive NADH : Q_6 oxidoreductase from mitochondria of *Saccharomyces cerevisiae*. *Eur J Biochem* **176**: 377–341.

Eschemann A, Galkin A, Oettmeier W, Brandt U & Kerscher S (2005) HDQ (1-hydroxy-2-dodecyl-4(1*H*)quinolone), a high affinity inhibitor for mitochondrial alternative NADH dehydrogenase: evidence for a ping-pong mechanism. *J Biol Chem* **280**: 3138–3142.

Fisher N, Bray PG, Ward SA & Biagini GA (2007) The malaria parasite type II NADH : quinone oxidoreductase: an alternative enzyme for an alternative lifestyle. *Trends Parasitol* **23**: 305–310.

Fry M, Webb E & Pudney M (1990) Effect of mitochondrial inhibitors on adenosine triphosphate levels in *Plasmodium falciparum*. *Comp Biochem Physiol* **B96**: 775–782.

Izumiya N, Kato T, Aoyaga H, Waki M & Kondo M (1979) *Synthetic Aspects of Biologically Active Cyclic Peptides: Gramicidin S and Tyrocidines*. Halsted Press, New York.

Johnson D & Lardy H (1967) Isolation of liver or kidney mitochondria. *Methods in Enzymology, Vol. 10* (Estabrook RW & Pullman ME, eds), pp. 94–96. Academic Press, New York.

Johnson LE & Dietz A (1971) Scopafungin, a crystalline antibiotic produced by *Streptomyces hygroscopicus* var. *enhygrus* var. *nova*. *Appl Microbiol* **22**: 303–308.

Kana BD, Weinstein EA, Avarbock D, Dawes SS, Rubin H & Mizrahi V (2001) Characterization of the *cydAB*-encoded cytochrome *bd* oxidase from *Mycobacterium smegmatis*. *J Bacteriol* **183**: 7076–7086.

Kerscher SJ (2000) Diversity and origin of alternative NADH : ubiquinone oxidoreductase. *Biochim Biophys Acta* **1459**: 274–283.

Kerscher SJ, Okun JG & Brandt U (1999) A single external enzyme confers alternative NADH : ubiquinone oxidoreductase activity in *Yarrowia lipolytica*. *J Cell Sci* **112**: 2347–2354.

Kondejewski LH, Farmer SW, Wishart D, Kay CM, Hancock REW & Hodges RS (1996) Modulation of structure and antibacterial and hemolytic activity by ring size in cyclic gramicidin S analogs. *J Biol Chem* **271**: 25261–25268.

Matsushita K, Shinagawa E, Adachi O & Ameyama M (1987) Purification and characterization of cytochrome *o*-type oxidase from *Gluconobacter suboxydans*. *Biochim Biophys Acta* **894**: 304–312.

Matsushita K, Toyama H & Adachi O (1994) Respiratory chains and bioenergetics of acetic acid bacteria. *Advances in Microbial Physiology, Vol. 36* (Rose AH & Tempest DW, eds), pp. 247–301. Academic Press Ltd, London.

Miyoshi H, Takegami K, Sakamoto K, Mogi T & Iwamura H (1999) Characterization of the ubiquinol oxidation sites in cytochromes *bo* and *bd* from *Escherichia coli* using aurachin C analogues. *J Biochem* **125**: 138–142.

Mogi T, Ui H, Shiomi K, Ōmura S & Kit K (2008) Gramicidin S identified as a potent inhibitor for cytochrome *bd*-type quinol oxidase. *FEBS Lett* **582**: 2299–2302.

Prenner EJ, Lewis RNAH, Newman KC, Gruner SM, Kondejewski LH, Hodges RS & McElhaney RN (1997) Nonlamellar phases induced by the interaction of gramicidin S with lipid bilayers. A possible relationship to membrane disrupting activity. *Biochemistry* **36**: 7906–7916.

Prust C, Hoffmeister M, Liesegang H, Wiezer A, Fricke WF, Ehrenreich A, Gottschalk G & Deppenmeier U (2005) Complete genome sequence of the acetic acid bacterium *Gluconobacter oxydans*. *Nat Biotechnol* **23**: 195–200.

Saleh A, Friesen J, Baumeister S, Gross G & Bohne W (2007) Growth inhibition of *Toxoplasma gondii* and *Plasmodium falciparum* by nanomolar concentrations of 1-hydroxy-2-dodecyl-4(1*H*)quinolone, a high-affinity inhibitor of alternative (type II) NADH dehydrogenases. *Antimicrob Agents Ch* **51**: 1217–1222.

Shi L, Sohaskey CD, Kana BD, Dawes S, North RJ, Mizrahi V & Gennaro ML (2005) Changes in energy metabolism of *Mycobacterium tuberculosis* in mouse lung and under *in vitro* conditions affecting aerobic respiration. *P Natl Acad Sci USA* **102**: 15629–15634.

Takashima E, Takamiya S, Takeo S, Mi-ichia F, Amino H & Kita K (2001) Isolation of mitochondria from *Plasmodium falciparum* showing dihydroorotate dependent respiration. *Parasitol Int* **50**: 273–278.

Ui H, Ishiyama A, Sekiguchi H, Namatame M, Nishihara A, Takahashi A, Shiomi K, Otoguro K & Ōmura S (2007) Selective and potent *in vitro* antimalarial activities found in four microbial metabolites. *J Antibiot* **60**: 220–222.

Yamashita T, Nakamaru-Ogiso E, Miyoshi H, Matsuo-Yagi A & Yagi T (2007) Roles of bound quinone in the single subunit NADH–quinone oxidoreductase (Ndi1) from *Saccharomyces cerevisiae*. *J Biol Chem* **282**: 6012–6020.

Yano T, Li L-S, Weinstein E, The J-S & Rubin H (2006) Steady-state kinetics and inhibitory action of antitubercular phenothiazines on *Mycobacterium tuberculosis* type-II NADH-menaquinone oxidoreductase (NDH-2). *J Biol Chem* **281**: 11456–11463.

J. Biochem. 2009;145(2)229–237
doi:10.1093/jb/mvn161

Mitochondrial Dehydrogenases in the Aerobic Respiratory Chain of the Rodent Malaria Parasite *Plasmodium yoelii yoelii*

Kenji Kawahara[1], Tatsushi Mogi[1,*], Takeshi Q Tanaka[1], Masayuki Hata[1], Hideto Miyoshi[2] and Kiyoshi Kita[1,†]

[1]Department of Biomedical Chemistry, Graduate School of Medicine, the University of Tokyo, Hongo, Bunkyo-ku, Tokyo 113-0033; and [2]Division of Applied Life Sciences, Graduate School of Agriculture, Kyoto University, Sakyo-ku, Kyoto 606-8502, Japan

Received October 7, 2008; accepted November 19, 2008; published online December 6, 2008

In the intraerythrocytic stages of malaria parasites, mitochondria lack obvious cristae and are assumed to derive energy through glycolysis. For understanding of parasite energy metabolism in mammalian hosts, we isolated rodent malaria mitochondria from *Plasmodium yoelii yoelii* grown in mice. As potential targets for antiplasmodial agents, we characterized two respiratory dehydrogenases, succinate:ubiquinone reductase (complex II) and alternative NADH dehydrogenase (NDH-II), which is absent in mammalian mitochondria. We found that *P. y. yoelii* complex II was a four-subunit enzyme and that kinetic properties were similar to those of mammalian enzymes, indicating that the *Plasmodium* complex II is favourable in catalysing the forward reaction of tricarboxylic acid cycle. Notably, *Plasmodium* complex II showed IC_{50} value for atpenin A5 three-order of magnitudes higher than those of mammalian enzymes. Divergence of protist membrane anchor subunits from eukaryotic orthologs likely affects the inhibitor resistance. Kinetic properties and sensitivity to 2-heptyl-4-hydroxyquinoline-*N*-oxide and aurachin C of NADH: ubiquinone reductase activity of *Plasmodium* NDH-II were similar to those of plant and fungus enzymes but it can oxidize NADPH and deamino-NADH. Our findings are consistent with the notion that rodent malaria mitochondria are fully capable of oxidative phosphorylation and that these mitochondrial enzymes are potential targets for new antiplasmodials.

Key words: complex II, inhibitor, mitochondria, NDH-II, rodent malaria.

Abbreviations: AC, aurachin C; DCIP, 2,4-dichlorophenolindophenol; DHO, dihydroorotate; DHOD, DHO dehydrogenase; HQNO, 2-heptyl-4-hydroxyquinoline-*N*-oxide; hrCNE, high-resolution clear-native electrophoresis; IC_{50}, the 50% inhibitory concentration; NBT, nitro blue tetrazolium chloride; NDE, NDH-II bound to the outer surface of the mitochondrial inner membrane; NDI, NDH-II bound to the matrix side of the mitochondrial inner membrane; NQR, NADH:quinone reductase; Q_n, ubiquinone-n; SDH, succinate dehydrogenase; SQR, succinate:quinone reductase; TCA, tricarboxylic acid.

INTRODUCTION

Malaria remains one of the main global health problems, causing more than 1 million deaths per year, with about 90% of deaths and 60% of cases occurring in Africa, south of the Sahara (*1*). Mortality associated with malaria is mainly caused by the erythrocytic stage cells of human malaria *Plasmodium falciparum*. The emerging resistance against established drugs in *Plasmodium* populations (*2*) emphasizes the urgent need for the development of new antiplasmodial drugs.

Energy metabolism of *Plasmodium* is quite different from that of mammalian hosts. Intraerythrocytic stages of parasites have been considered for a long time to rely on incomplete oxidation of glucose with secretion of end products such as lactate and pyruvate (*3*) and to possess mitochondria that lack oxidative phosphorylation and a functional tricarboxylic acid (TCA) cycle (*4*, *5*). *Plasmodium* spp. lacks genes coded for the proton-translocating NADH dehydrogenase (NDH-I, complex I) present in mammalian mitochondria (*6*, *7*) and uses a rotenone-insensitive single-subunit NADH dehydrogenase (NDH-II) (*8*), which is assumed not to oxidize deamino-NADH (*9*). Succinate:ubiquinone oxidoreductase (complex II, succinate dehydrogenase (SDH)) is a membrane-bound TCA cycle enzyme and consists of four subunits: a flavoprotein subunit (Fp, SDH1) and an iron–sulphur subunit (Ip, SDH2) form a soluble heterodimer, which binds to a membrane anchor *b*-type cytochrome [CybL (SDH3)/CybS (SDH4) heterodimer]. The *Plasmodium SDH1* and *SDH2* genes have been cloned by homology probing (*10*) while SDH3 and SDH4 appear highly divergent from orthologs and are still not annotated in the current database (*6*, *7*). Membrane bound subuniuts *a* and *b* of ATP synthase also remain unidentified (*6*, *7*), and thus complete mitochondrial ATP synthase was assumed to be absent in *Plasmodium* spp. (*4*, *5*, *11–13*). Recently, Painter *et al.* (*13*) claimed that

*To whom correspondence addressed. Tel: +81-3-5841-3526, Fax: +81-3-5841-3444, E-mail: tmogi@m.u-tokyo.ac.jp
†Correspondence may also be addressed. Tel: +81-3-5841-3526, Fax: +81-3-5841-3444, E-mail: kitak@m.u-tokyo.ac.jp

the mitochondrial respiratory chain is required only for the regeneration of an oxidized form of ubiquinone, which serves as the electron acceptor for type 2 dihydroorotate dehydrogenase (DHOD), an essential enzyme for pyrimidine biosynthesis. It is widely accepted that the majority of the parasite's ATP demand is met through glycolysis (*11*).

On the contrary, atovaquone, an inhibitor for ubiquinol:cytochrome *c* reductase (complex III) (*14*), showed the antiplasmodial activity for *P. falciparum* with the 50% inhibitory concentration (IC_{50}) of 1 nM (*15*) and collapsed the mitochondrial membrane potential in *P. yoelii yoelii* (*16*). Uyemura *et al.* (*8*, *17*) demonstrated oxidative phosphorylation and succinate respiration in trophozoites of rodent malaria parasites. These observations suggest that *Plasmodium* mitochondria possess all subunits for canonical complex II and ATP synthase and are fully capable of oxidative phosphorylation.

It was shown recently that metabolism in *P. falciparum* parasites grown in human patients is affected by varied oxygen and substrate levels and by host-parasite interactions (*18*). The authors found the induction of gene sets associated with oxidative phosphorylation including respiratory enzymes. For understanding energy metabolism in malaria parasites, the isolation of active mitochondria from parasites, which have been adapted to host environments, is essential. In this study, *P. y. yoelii* mitochondria were isolated from parasites grown in mouse erythrocytes and enzymatic properties of complex II and NDH-II were characterized. Two-dimensional PAGE analysis supports the presence of membrane anchors in *Plasmodium* complex II. These findings indicate that *Plasmodium* mitochondria are fully capable of succinate-dependent oxidative phosphorylation as suggested by previous observations (*8*, *17*). Because the difference in the inhibitor sensitivity of complex II between *Plsamodium* and mammalian enzymes and the absence of NDH-II in mammalian mitochondria, these two enzymes are promising targets for new antimaralials.

MATERIALS AND METHODS

Parasite Culture—Animal care and experimental procedures were performed according to the Guidelines for Animal Experimentation, the University of Tokyo. *P. y. yoelii* strain 17XL was a kind gift of H. Otsuki (Ehime University). This strain can rapidly propagate without cerebral malaria and does not infect reticulocytes. About 3.0×10^7 parasites were injected intraperitoneally to 8-week-old female BALB/c mice, and the developmental stage and parasitemia were monitored by examination of Giemsa-stained thin blood smears. About 7.5 ml of the blood was collected from 10 mice by cardiac puncture 130–140 h after infection. To remove leukocytes and platelets, the blood was mixed with 0.5 ml of heparine and passed over a powdered cellulose column (CF11; Whatman, Clifton; 0.5 ml/ml blood), which has been equilibrated with 20 ml of PBS (*19*). Erythrocytes were eluted with 30 ml of PBS and collected by centrifugation at 4°C at $800 \times g$ for 5 min. In control experiments with uninfected mice, microscopic observations and examination of complex II and dihydroorotate dehydrogenase (DHOD) activities excluded the possible contamination of mouse leukocytes in the eluate. Erythrocytes were washed three times with RPMI-1640 medium (Gibco) and then transferred to RPMI-1640 medium supplemented with 10% AlbuMax I (Gibco) at the hematoclit of 3%. Then erythrocytes were incubated at 37°C for 2 h under conditions of 90% N_2, 5% O_2 and 5% CO_2, and trophozoite-rich parasites were recovered by centrifugation as above.

Preparation of Mitochondria—To isolate parasites, infected erythrocytes were lysed for 10 min on ice with 0.1% (w/v) saponin and the lysate was centrifuged at 4°C at $2,380 \times g$ for 10 min to remove erythrocyte membranes. Parasites were washed twice with PBS by centrifugation at 4°C at $5,800 \times g$ for 10 min and resuspended with 10–20 ml of buffer A [225 mM mannitol, 75 mM sucrose, 5 mM $MgCl_2$, 5 mM KH_2PO_4, 5 mM HEPES, 1 mM EGTA (pH 7.4)], supplemented with 0.1% (w/v) fatty acid-free bovine serum albumin (PAA Cell Culture Co.), 1 mM phenylmethanesufonyl fluoride (Sigma) and 1 × Protease Inhibitor Cocktail for general use (Sigma). Parasites were disrupted by N_2 cavitation at 1,200 psi for 20 min with 4639 Cell Disruption Bomb (Parr, USA) (*20*). Lysate was centrifuge at 4°C at $700 \times g$ for 8 min, and the resultant precipitate containing unbroken parasites was resuspended with 10 ml of buffer A and disrupted as above. This procedure was repeated twice to improve the parasite yield. Crude mitochondria were recovered from the supernatant by centrifugation at 4°C at $10,000 \times g$ for 8 min and suspended in buffer A at ~5 mg protein/ml. Rat liver mitochondria were prepared as described by Johnson and Lardy (*21*).

Enzyme Assay—Enzyme assay was performed at 25°C with V-660 double monochromatic spectrophotometer (JASCO, Tokyo, Japan; <0.00005 Abs noise) or UV-3000 double wavelength spectrophotometer (Shimadzu Corp., Kyoto, Japan), and reactions were started by addition of substrates (electron donors). Succinate:quinone reductase (SQR) activity was determined as quinone-mediated succinate:2,4-dichlorophenolindophenol (DCIP) reductase in 50 mM potassium phosphate (pH 8.0) containing 10 mM potassium succinate, 100 μM ubiquinone-2 (Q_2) and 45 μM DCIP ($\varepsilon_{600} = 21\ mM^{-1}\ cm^{-1}$) in the presence of 2 mM KCN. NADH:ubiquinone reductase (NQR) activity was measured in 50 mM potassium phosphate (pH 8.0) containing 200 μM NADH ($\varepsilon_{340} = 6.22\ mM^{-1}\ cm^{-1}$) and 100 μM ubiquinone-1 (Q_1) in the presence of 10 μM atovaquone and 2 mM KCN (*15*). DHOD activity was measured as DHO:DCIP reductase in 30 mM Tris–HCl (pH 8.0) containing 500 μM DHO, 100 μM Q_2 and 45 μM DCIP in the presence of 2 mM KCN (*20*). DHO: cytochrome *c* reductase activity was determined with 20 μM horse cytochrome *c* ($\varepsilon_{550} = 19\ mM^{-1}\ cm^{-1}$) in place of 45 μM DCIP (*20*). For inhibition studies, the reaction mixture was preincubated for 5 min in the presence of 0.1% (w/v) sucrose monolaurate (Mitsubishi-Kagaku Foods Co., Tokyo, Japan) to disperse hydrophobic substrates and inhibitors. Kinetic analysis and the estimation of the 50% inhibitory concentration (IC_{50}) were performed as described previously (*22*).

Clear-Native Electrophoresis and Activity Staining—Mitochondria were precipitated at 4°C at 20,400 × *g* for 5 min and resuspended at 6 mg protein/ml in 10 mM Tris–HCl (pH 7.4) containing 1% sucrose monolaurate, 1 mM sodium malonate and Protease Inhibitor Cocktail by brief sonication. After 20 min incubation at 4°C with rotating, the mixture was centrifuged at 4°C at 107,000 × *g* for 30 min and supernatant was concentrated at 4°C at 4,000 × *g* with Nanosep ultrafiltration devices (MWCO 100,000, Pall Life Science). Solubilized mitochondrial proteins were subjected to high resolution clear-native electrophoresis (hrCNE) (*23*) with 3–12% Novex gels (Invitrogen) using 0.02% dodecylmaltoside and 0.05% sodium deoxycholate for the cathode buffer additives. Gels were incubated at 25°C for 10 min in 30 mM Tris–HCl (pH 7.4) containing 20 mM potassium succinate and 0.5 mM nitro blue tetrazolium chloride (NBT), and then complex II band was visualized by 1 h incubation in dark in the presence of 0.2 mg/ml phenazine methosulphate. Protein bands were stained with GelCode (Pierce).

Analysis of Membrane Anchor Subunits of Complex II—Complex II bands identified as succinate:NBT reductase in hrCNE were cut out from gels and equilibrated with an equal amount of 2× SDS–PAGE sample buffer. Gel pieces were applied to 10–20% Supersep gels (Wako Pure Chemicals, Tokyo, Japan) and SDS–PAGE analysis was carried out. Protein bands were visualized by silver staining.

Miscellaneous—Protein contents of mitochondria and solubilized membrane proteins were determined with BIO-RAD and BCA protein assay reagent (Pierce), respectively, using bovine serum albumin as standard. Western blot analysis was carried out using anti-*P. falcifaum* (Pf) Fp and anti-PfIp rabbit antiserum and cross-reacted bands were visualized by alkaline phosphatase-conjugated anti-rabbit IgG (Bio-Rad) *(24)*.

RESULTS

Preparation of Plasmodium Mitochondria—After infection of mice with rodent malaria parasites, we monitored amounts of erythrocytes and parasitemia and found that the number of parasites decreased sharply 140 h after infection as the number of the erythrocyte decreased. Thus, we collected the infected blood 130 to 140 h after infection. Leukocyte-free washed erythrocytes were incubated at 37°C for 2 h in RPMI-1640 medium supplemented with 10% AlbuMax I to adjust the developmental stage to trophozoites (trophozoite : ring : schizont = 7 : 2 : 1). Then the parasites were released from infected erythrocytes with 0.1% saponin and disrupted by the N_2 cavitation method (*20*).

Yield of Plasmodium Mitochondria—SQR activity and DHOD activity of *P. y. yoelii* mitochondria were 5- and 3-fold, respectively, higher than those of the axenic cultured *P. falciparum* (*20*). Furthermore, yields of mitochondrial proteins (5.5 ± 1.3 mg protein) and total activities of complex II (56 ± 14 mU) and DHOD (132 ± 18 mU) after preparation from ten infected mice were much greater than those of *P. falciparum* mitochondria [1 mg protein, 2 mU (*25*), and 7 mU (*20*), respectively, from the 360-ml *in vitro* culture]. Thus, in terms of the yield and specific activity, *P. y. yoelii* mitochondria are suitable for biochemical studies on mitochondrial enzymes of malaria parasites.

Table 1. **Enzymatic properties of *P. y. yoelii* mitochondria.**

Enzyme	Specific activity (mU/mg protein)	
	P. y. yoelii[a]	Rat liver
Succinate:DCIP reductase (complex II)	2.66 ± 0.02	188
NADH:Q_1 reductase[b]	42.2 ± 0.3	152
NADH:Cyt *c* reductase[c]	18.6 ± 1.6	ND[d]
DHO:DCIP reductase (DHOD)	10.5 ± 1.3	2.6
Q_1H_2 oxidase (complex III + complex IV)	19.4 ± 0.2	166

[a]Values were mean ± SD. Freshly prepared *P. y. yoelii* mitochondria showed SQR, NQR and DHOD activities of 10.2 ± 0.1, 63.2 ± 10.1 and 24.1 ± 3.9 mU/mg protein (n = 6), respectively. Enzyme activities were reduced to about one half after freeze-thaw of mitochondria preparations, which have been stored at −80°C. [b]NDH-II of *P. y. yoelii* or NDH-I of rat liver mitochondria were analysed. [c](NDH-II of *P. y. yoelii* or NDH-I of rat liver mitochondria) + complex III were analysed. [d]ND, not determined.

Comparison of Mitochondrial Enzymes from P. y. yoelii and Rat Liver—When comparing with rat liver mitochondria, SQR (complex II), NQR (NDH-II) and Q_1H_2 oxidase (complex III *plus* complex IV) activity of *P. y. yoelii* mitochondria were 1.4%, 28% and 12%, respectively, of rat liver mitochondria whereas DHOD activity was 4-fold higher than that of rat liver mitochondria (Table 1). Rotenone [IC_{50} = 13 nM for bovine complex I (*26*)] inhibited rat liver mitochondria complex I 95–97% at 1 μM while the inhibition of the *P. y. yoelli* NQR activity by 10 μM rotenone was only 20%. Since NQR activity of *P. y. yoelii* mitochondria followed a simple Michaelis–Menten kinetics (see below), we concluded that the enzyme activities are not due to contaminated mouse mitochondria derived from leukocytes or platelets.

Enzymatic Properties of Plasmodium Complex II—SQR activity of *P. y. yoelii* mitochondria displayed Michaelis–Menten kinetics (Fig. 1). Apparent K_m values for succinate and Q_2 were estimated to be 49 and 0.17 μM, respectively, which are close to 20 and 0.5 μM, respectively, of bovine complex II (*27*). Apparent K_m value for Q_1 was found to be 1.6 μM. Differences in K_m value (9-fold) and V_{max}/K_m ratio (19-fold) between Q_1 and Q_2 indicate that the 6-polyprenyl tail of the ubiquinone ring contributes to the binding affinity and that Q_2 is better substrate than Q_1.

Then effects of the quinone-binding site inhibitors on the SQR activity were examined. Atpenin A5 and carboxin are known inhibitors for bovine complex II with IC_{50} values of 4 nM and 1 μM, respectively (*28*) and plumbagin (5-hydroxy-2-methyl-1,4-naphthoquinone) has been reported to inhibit *P. falciparum* complex II (IC_{50} = 5 μM) and the growth (IC_{50} = 0.27 μM) (*29*). At 100 μM Q_2, we found that IC_{50} values for atpenin A5 and carboxin were 4.6 and 3.6 μM, respectively, in *P. y. yoelii* mitochondria and 7.1 nM and 3.8 μM, respectively, in rat liver mitochondria (Fig. 2). The inhibition by plumbagin was only 50% even at 100 μM.

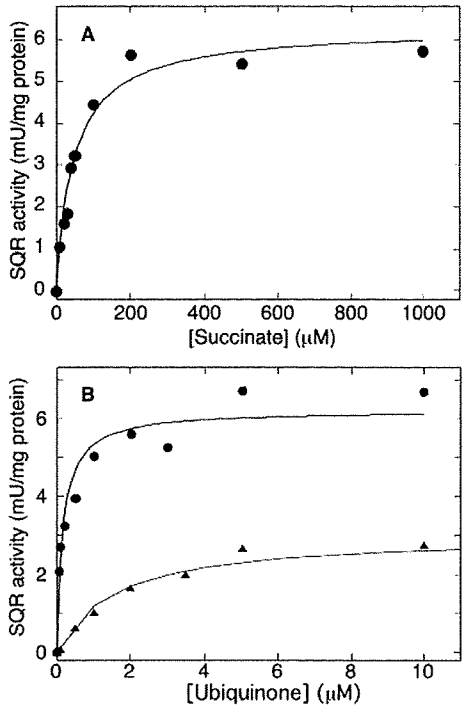

Fig. 1. **Kinetic analysis of SQR activity of *P. y. yoelii* mitochondria.** (A) As a function of the succinate concentration, SQR activity was examined at 6 μg mitochondrial protein/ml in the presence of 0.1 mM Q_2. Data points were averages from three independent preparations (6.19 ± 0.93 mU/mg protein with 1 mM succinate and 0.1 mM Q_2). Data were fitted to Michaelis–Menten kinetics with apparent K_m and V_{max} values of 49.3 ± 7.0 μM and 6.26 ± 0.27 mU/mg protein, respectively. (B) As a function of the Q_1 (circles) or Q_2 (triangles) concentration, SQR activity was examined in the presence of 10 mM succinate. Data points were averages from two independent preparations (6.25 ± 0.87 mU/mg protein with 1 mM succinate and 0.1 mM Q_2). Data were fitted to Michaelis–Menten kinetics with apparent K_m and V_{max} values of 1.61 ± 0.20 μM and 3.03 ± 0.12 mU/mg protein, respectively, for Q_1 and 0.17 ± 0.04 μM and 6.20 ± 0.30 mU/mg protein, respectively, for Q_2.

Membrane Anchor Subunits of Plasmodium Complex II—For reduction of ubiquinone, *Plasmodium* complex II should have a quinone-binding pocket provided by Ip and the CybL/CybS heterodimer (*30–32*). For the examination of subunit structure of *Plasmodium* complex II, we first determined the molecular weight of *P. y. yoelii* complex II by hrCNE, followed by in-gel activity staining as phenazine methosulphate-mediated succinate : NBT reductase. An apparent molecular weight of *P. y. yoelii* complex II was estimated to be 135 kDa (Fig. 3, lane 2), which is comparable to 130 kDa of bovine and yeast complex II (*33*). Western blot analysis identified Fp and Ip as the 70- and 35-kDa proteins, respectively (Fig. 3, lanes 3 and 4), indicating that a sum of molecular weights of membrane anchor subunits is about 30 kDa. Subsequently, the 135-kDa bands in hrCNE were excised from gels and subjected to SDS–PAGE analysis. Due to an extremely low activity of *Plasmodium* complex II (~1% of mammalian mitochondria) and the diffusion of

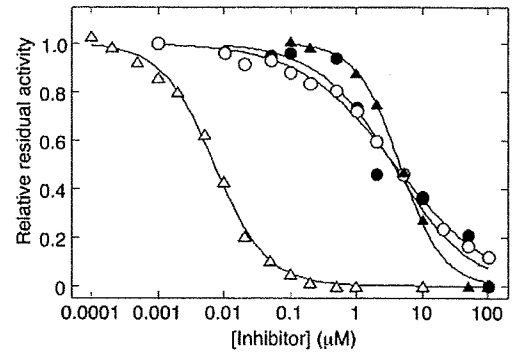

Fig. 2. **Inhibition of SQR activity of *P. y. yoelii* mitochondria by atpenin A5 and carboxin.** SQR activity of *P. y. yoelii* (closed symbols) and rat liver (open symbols) mitochondria was determined with 10 mM potassium succinate and 0.1 mM Q_2 in the presence of atpenin A5 (triangles), and carboxin (circles). Data points were average values from two independent preparations. IC_{50} values were determined to be 4.6 ± 0.2 μM for atpenin A5 and 3.6 ± 1.0 μM for carboxin in *P. y. yoelii* mitochondria and 7.1 ± 0.3 nM for atpenin A5 and 3.8 ± 0.1 μM for carboxin in rat liver mitochondria. Control activitiy of *P. y. yoelii* mitochondria was 2.68 ± 0.03 mU/mg protein.

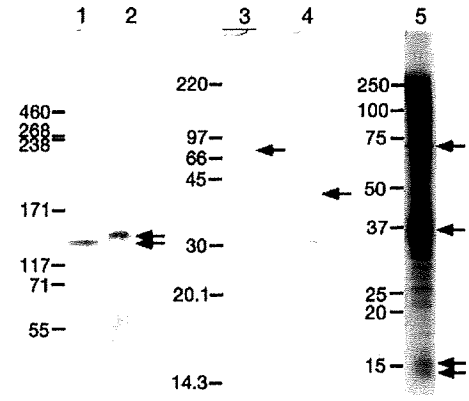

Fig. 3. **Electrophoresis analysis of complex II in *P. y. yoelii* mitochondria.** Solubilized mitochondrial proteins were subjected to hrCNE, and complex II of bovine (lane 1, 2.4 μg protein) and *P. y. yoelii* (lane 2, ~0.4 mg protein) mitochondria were visualized by SDH activity staining. Arrows indicate complex II bands. For Western blot analysis, 10 μg of mitochondrial proteins were subjected to 15% SDS–PAGE and Fp (lane 3) and Ip (lane 4), indicated by arrows, were identified by anti-PfFp and anti-PfIp rabbit antisera, respectively. For identification of *P. y. yoelii* complex II subunits, complex II bands in hrCNE were excised from gels and subjected to 10–20% SDS–PAGE, followed by silver staining (lane 5). Putative subunits of *P. y. yoelii* complex II are indicated by arrows. HiMark Prestained High Molecular Weight Protein Standard (Invitrogen), Rainbow Colored Protein Molecular Weight Marker (High molecular weight range) (Amersham Pharmacia Biotech), and Precision Plus Protein Standard (Bio-Rad) were used as molecular weight standards for lanes 1 and 2, lanes 3 and 4, and lane 5, respectively.

a reduced product of NBT, it was difficult to cut out the complex II band but we were able to identify 70, 35, 16 and 14 kDa bands as putative subunits of the 135-kDa complex (Fig. 3, lane 5).

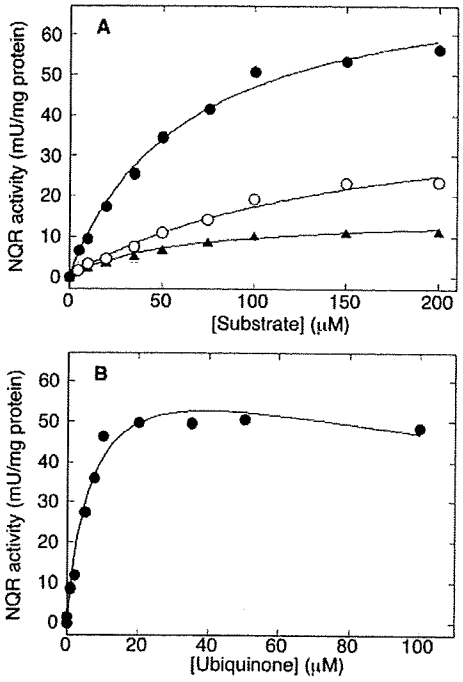

Fig. 4. **Kinetic analysis of NQR activity in *P. y. yoelii* mitochondria.** (A) As a function of the concentration of NADH (closed circle), NADPH (open circle) or deamino-NADH (closed triangle), NQR activity was examined at 6 μg protein/ml in the presence of 0.1 mM Q_1. Data points were averages from two independent preparations (44.9 ± 4.8 mU/mg protein with 0.2 mM NADH). Data were fitted to Michaelis–Menten kinetics with apparent K_m and V_{max} values of 63.2 ± 6.9 μM and 76.7 ± 3.4 mU/mg protein, respectively, for NADH, 157 ± 33 μM and 44.4 ± 5.4 mU/mg protein, respectively, for NADPH, 58.4 ± 5.7 μM and 15.1 ± 0.6 mU/mg protein, respectively, for deamino-NADH. (B) As a function of the concentration of Q_1, NQR activity was examined in the presence of 0.2 mM NADH. Data points were average values from two independent preparations [48.6 ± 7.9 mU/mg protein at 0.1 mM Q_1). Data were fitted to substrate inhibition kinetics with apparent K_m, V_{max} and K_{is} values of 7.2 ± 1.7 μM, 71.8 ± 7.6 mU/mg protein, and 218 ± 97 μM, respectively, using the equation $v = V_{max}\, S/(K_m + S + S\,(1+S/K_{is}))$.

Enzymatic Properties of Plasmodium NDH-II—*Plasmodium* spp. lacks genes encoding complex I (*6*, *7*) and uses a single-subunit NADH dehydrogenase (NDH-II) (*8*, *15*). Upon permealization of mitochondria with 30 μg/ml alamethicin, which forms pores large enough to permit the rapid diffusion of NADH (*34*), NQR and SQR activities increased 32% and 27%, respectively, indicating that *Plasmodium* NDH-II is likely located at the matrix side of the inner membrane.

When reactions were started by addition of NADH, NQR activity showed a simple Michaelis–Menten kinetics with apparent K_m and V_{max} values of 63 μM for NADH and 77 mU/mg protein, respectively (Fig. 4A). K_m value for NADH was closer to 31 μM of *Saccharomyces cerevisiae* internal NDH-II (NDI1) (*35*) and 34 μM of *E. coli* NDH-II (*36*) than 15 μM of yeast *Yarrowia lipolytica* external NDH-II (NDE) (*37*). In contrast,

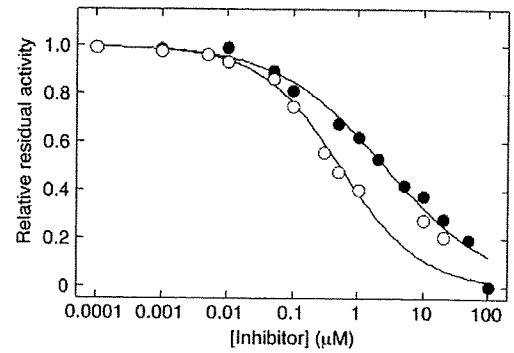

Fig. 5. **Inhibition of NQR activity of *P. y. yoelii* mitochondria by HQNO and Aurachin C1-10.** NQR activity of *P. y. yoelii* mitochondria was determined with 0.2 mM NADH and 0.1 mM Q_1 in the presence of HQNO (closed circle) or aurachin C1-10 (open circle). Data points were average values from two independent preparations. Control activity of *P. y. yoelii* mitochondria was 45.6 ± 1.3 mU/mg protein with 0.1 mM Q_1. IC_{50} values for HQNO and aurachin C1-10 were estimated to be 2.5 ± 0.4 and 0.47 ± 0.03 μM, respectively.

Q_1-started NQR activity showed substrate inhibition kinetics with K_m and K_{is} values of 7 and 218 μM, respectively, for Q_1 (Fig. 4B). Unlike *E. coli* NADH-II (*36*) and *Y. lipolytica* NDE (*37*), *P. y. yoelii* NDH-II can oxidize deamino-NADH (K_m = 58 μM, V_{max} = 15 U/mg protein) and NADPH (K_m = 157 μM, V_{max} = 44 mU/mg protein) (Fig. 5A). V_{max}/K_m ratios indicate that *Plasmodium* NDH-II is more specific to NADH compared to NAD(P)H dehydrogenases from red beet root mitochondria [NDI (*38*) and NDE (*39*)].

Since mammalian hosts lack NDH-II, this enzyme is a promising target for new antiplasmodial agents. However, inhibitors for NDH-II are rare and mostly unspecific (*34*). Fry *et al.* (*11*) examined effects of inhibitors on ATP level in erythrocytic *P. falciparum* and found that 2-heptyl-4-hydroxyquinoline *N*-oxide (HQNO) and 5-hydroxy-2-methyl-1,4-naphthoquinone (plumbagin) showed antimalarial activities with IC_{50} values of 4.0 and 3.5 μM, respectively. In yeast, quinolone analogues HQNO and aurachin C 0-11 were shown to inhibit NDI1 with the IC_{50} values of 8 and 0.2 μM, respectively (*40*). In this study, we examined effects of HQNO and aurachin C 1-10 (*41*) on NADH:Q_1 reductase activity and determined IC_{50} values to be 2.5 and 0.5 μM, respectively (Fig. 5). Our data indicate that the quinolone analogues are potent inhibitors for *Plasmodium* NDH-II. Trifluoroperazine, the uncompetitive inhibitor in terms of Q_2 for *Mycobacterium tuberculosis* NDH-II (IC_{50} = 12 μM) (*42*), reduced the NADH:Q_1 reductase activity to 26% of the control at 100 μM.

DISCUSSION

Properties of Plasmodium Complex II—Parasitic nematodes adapted to hypoxic host environments, have modified respiratory chain, where isoforms of complex II serve as fumarate reductase (*43*, *44*). Kinetic properties of *P. y. yoelii* complex II are similar to those of mammalian enzymes and thus suitable for catalysing the

Table 2. **Effects of quinone-binding site inhibitors on SQR activity of *P. y. yoelii* mitochondria.**

100 μM inhibitor	*P. y. yoelii* mitochondria	Rat liver mitochondria
Control	100%	100%
Atpenin A5	<0.4	<0.05
Carboxin	<0.4	<0.05
Flutoranil	58	22
TTFA	80	12
HQNO	54	94
Plumbagin	52	98
DNP-17	67	99

Control activities (mean ± SD) were 2.66 ± 0.02 (*P. y. yoelii*) and 180 ± 5 (rat liver) mU/mg protein.

forward reaction of TCA cycle (i.e. the oxidation of succinate). It should be noted that *Plasmodium* complex II was more resistant to known quinone-binding site inhibitors for mammalian complex II (Table 2), probably due to the divergence of membrane anchor subunits of *Plasmodium* complex II.

From the whole cell lysate of *P. falciparum*, Suraveratum *et al.* (*28*) purified complex II as the Fp/Ip heterodimer with an apparent molecular weight of 90 kDa and claimed that it has a much lower K_m value (3 μM) for succinate and plumbagin-sensitive SQR activity. However, the concentration (0.2%) of octyl glucoside used for the isolation of *P. falciparum* complex II was not enough for the solubilization of membrane proteins (i.e. critical micell concentration of octyl glucoside is 0.73%). Octyl glucoside likely dissociates the Fp/Ip dimer from the membrane anchor and the aerobic isolation of the Fp/Ip dimer would damage the iron–sulphur clusters in Ip. Thus, SQR activity of such preparations need to be carefully examined.

Plasmodium CybL and CybS are still not annotated in the current database (*6*, *7*), likely due to the divergence from ortholog sequences. However, 2D–PAGE analysis (Fig. 3), SQR activity (Fig. 1, refs. *20*, *25*) and the structure of quinone-binding site in complex II (*30–32*) support the presence of these membrane anchor subunits in *Plasmodium* spp. In membrane anchors of complex II, "$Rx_{16}Sx_2HR$" (helix I) and '$YHx_{10}D$' (helix II) motifs in CybL and '$LHx_{10}DY$' (helix II) motif in CybS are conserved for quinone/haem binding. And only such motifs are conserved in protist membrane anchors (*45*). One candidates for *P. y. yoelii* CybL (accession no. XP_731082, 10,086 Da) and one candidate for CybS (accession no. XP_726783, 10,379 Da) can be identified from 3,310 ORFs shared by *P. falciparum* and *P. y. yoelii* on the basis of the size (<200 amino acid residues), the presence of transmembrane segments (≤3), and the quinone/haem-binding motifs. PyCybL and PyCybS have two transmembrane regions and contain the quinone/haem-binding motifs, '$Rx_{14}Sx_2HY$' and '$YYx_{10}DY$' motifs and '$Yx_{10}G$' motif, respectively. In *S. cerevisiae* strain S288C (Baker's yeast), CybS (accession no. NP_010463) uses the $Yx_{10}DY$ motif, and the His-to-Tyr mutant of the CybL $YHx_{10}D$ motif retained a half of the enzyme activity and haem (*46*). Thus, in *Plasmodium* CybL and CybS, Tyr could also substitute the role of the conserved His residue in membrane anchor subunits. Although it has to be tested by protein chemically in future studies, our data support that the subunit structure of *Plasmodium* complex II is similar to that of mammalian complex II.

Properties of Plasmodium NDH-II—Previously, Krungkrai *et al.* (*47*) isolated mitochondrial complex I from *P. falciparum* and *P. berghei* as a 130-kDa complex containing 38- and 33-kDa subunits. They claimed that NADH:ubiquinone-8 reductase activity was sensitive to rotenone (IC_{50} = 12 μM) and plumbagin (IC_{50} = 6 μM). However, NDH-I is not encoded by the *Plasmodium* genomes (*6*, *7*) and concentrations of *n*-octyl glucoside used for the solubilization and purification were below its critical micelle concentration (CMC) where *n*-octyl glucoside cannot serve as a detergent. Alternative NADH dehydrogenase NDH-II is a rotenone-insensitive single-subunit enzyme (*15*, *34*) and the apparent molecular weights and subunit structure of *P. falciparum* (acc. no. XP_001352022 and MW 61,670) and *P. y. yoelii* (acc. no. XP_731423, MW 66,156) NDH-II are totally different from those reported by Krungkrai *et al.* (*47*). The IC_{50} value of mouse liver mitochondria for rotenone (8.4 μM; Table 3 in ref. 47) was three orders of magnitude higher than the IC_{50} reported for mammalian enzymes (*26*). Recently, Biagini *et al.* (*15*) used the whole cell lysate of *P. falciparum* and claimed that PfNDH-II was inhibited by diphenylene iodonium chloride (DPI, IC_{50} of 15–25 μM) and diphenyl iodonium chloride (IDP, IC_{50} = 66 μM). As pointed out by Vaidya *et al.* (*48*), the IC_{50} for the enzyme was 100- and 10-fold higher than those for the growth inhibition and other NADH oxidases in the lysate may contribute to the activity. Very recently, it was reported that purified recombinant PfNDH-II was not inhibited by known NDH-I inhibitors and flavoenzyme inhibitors (DPI and IDP) (Dong, C., Patel, V., Clardy, J., and Wirth, D., personal communication). Thus, previous studies on *Plasmodium* NDH-II need to be reexamined. Our data indicate that *Plasmodium* NDH-II is a member of internal NDH-II (Ndi), which reoxidizes NADH in the mitochondrial matrix. Recently, Saleh *et al.* (*49*) demonstrated the antiplasmodial activity (IC_{50} = 14 nM) of 1-hydroxy-2-dodecyl-4(1*H*)quinolone (HDQ), which has been identified as the potent inhibitor for *Y. lipolytica* NDE (IC_{50} = 0.2 μM) (*50*), demonstrating that *Plasmodium* NDH-II is a promising target for new drugs.

Oxidative Phosphorylation in Plasmodium Mitochondria—For a long time, it has been assumed that *Plasmodium* mitochondria cannot carry out oxidative phosphorylation (*4*, *5*) because of a lack of membrane anchor subunits of ATP synthase (*9*, *11*). Oxidative phosphorylation, succinate respiration (*8*, *17*), and effects of respiratory complex inhibitors on the generation of membrane potential (*16*) in rodent malaria mitochondria support the notion that *Plasmodium* mitochondria are fully capable of oxidative phosphorylation. Careful analysis of current genome databases (*6*, *7*) with partial subunits sequences of *Crithidia fasciculata* (*51*) and *Leishmania tarentolae* (*52*) could identify ten subunits of *P. falciparum* F_oF_1-ATP synthase, including membrane anchor subunits *a* (XP_001347344) and *b* (XP_001348969) (Mogi, T. and Kita, K., unpublished

results), which are found to be highly divergent from eukaryotic and bacterial counterparts. Thus, all canonical subunits of complex II and ATP synthase are present in *Plasmodium* spp., and malaria parasites can yield energy *via* oxidative phosphorylation. The *in vivo* expression profiles of parasites derived from infected patients showed the up-regulation of these enzymes under conditions similar to starvation in yeast (*18*).

CONCLUSION

We isolated active mitochondria from rodent malaria *P. y. yoelii* from infected mouse erythrocytes and characterized complex II and NDH-II. *Plasmodium* complex II is the four-subunit enzyme but its quinone-reduction site in the membrane anchor subunits seems structurally different from that of mammalian enzyme. *Plasmodium* NDH-II showed enzymatic properties similar to those of NDI and quinolones were found to be potent inhibitors. Alternative respiratory enzymes, which are absent in mammalian mitochondria, are as promising targets for new antibiotics (*53*, *54*). We hope that our findings will help understanding of energy metabolism in malaria parasites and the development of new antimalarial drugs.

FUNDING

This study was supported in part by a grant-in-aid for scientific research (20570124 to T.M.), scientific research on Priority Areas (18073004 to K.K.) and Creative Scientific Research (18GS0314 to K.K.) from the Japanese Ministry of Education, Science, Culture, Sports, and Technology. We thank Dr H. Ohtsuki (Ehime University) for *P. y. yoelii* strain 17XL, Dr. D. Wirth (Harvard School of Public Health) for the use of unpublished results prior to publication, and Ministry of Health, Labour and Welfare for financial supports.

CONFLICT OF INTEREST

None declared.

REFERENCES

1. World Health Organization (2007) Malaria Elimination. A field manual for low and moderate endemic countries. World Health Organization, Geneva, Switzerland
2. Hyde, J.E. (2005) Drug-resistant malaria. *Trends Parasitol.* **21**, 494–498
3. Sherman, I.W. (1998) Carbohydrate metabolism of asexual stages. in *Malaria, Parasite Biology, Pathogenesis and Protection* (Sherman, I.W., ed.), pp. 135–143, ASM Press, Washington, DC
4. Vaidya, A.B. (1998) Mitochondrial physiology as a target for atovaquone and other antimalarials. in *Malaria, Parasite Biology, Pathogenesis and Protection* (Sherman, I.W., ed.), pp. 355–368, ASM Press, Washington, DC
5. Van Dooren, G.G., Stimmler, L.M., and McFadden, G.I. (2006) Metabolic maps and functions of the *Plasmodium* mitochondrion. *FEMS Microbiol. Rev.* **30**, 596–630
6. Gardner, M.J., Hall, N., Fung, E., White, O., Berriman, M., Hyman, R.W., Carlton, J.M., Pain, A., Nelson, K.E., Bowman, S., Paulsen, I.T., James, K., Eisen, J.A., Rutherford, K., Salzberg, S.L., Craig, A., Kyes, S., Chan, M.S., Nene, V., Shallom, S.J., Suh, B., Peterson, J., Angiuoli, S., Pertea, M., Allen, J., Selengut, J., Haft, D., Mather, M.W., Vaidya, A.B., Martin, D.M., Fairlamb, A.H., Fraunholz, M.J., Roos, D.S., Ralph, S.A., McFadden, G.I., Cummings, L.M., Subramanian, G.M., Mungall, C., Venter, J.C., Carucci, D.J., Hoffman, S.L., Newbold, C., Davis, R.W., Fraser, C.M., and Barrell, B. (2002) Genome sequence of the human malaria parasite *Plasmodium falciparum*. *Nature* **419**, 498–511
7. Carlton, J.M., Angiuoli, S.V., Suh, B.B., Kooij, T.W., Pertea, M., Silva, J.C., Ermolaeva, M.D., Allen, J.E., Selengut, J.D., Koo, H.L., Peterson, J.D., Pop, M., Kosack, D.S., Shumway, M.F., Bidwell, S.L., Shallom, S.J., van Aken, S.E., Riedmuller, S.B., Feldblyum, T.V., Cho, J.K., Quackenbush, J., Sedegah, M., Shoaibi, A., Cummings, L.M., Florensk, L., Yatesk, J.R., Raine, J. D., Sinden, R.E., Harris, M.A., Cunningham, D.A., Preiser, P.R., Bergman, L.W., Vaidya, A.B., van Lin, L.H., Janse, C.J., Waters, A.P., Smith, H.O., White, O.R., Salzberg, S.L., Venter, J.C., Fraser, C.M., Hoffman, S.L., Gardner, M.J., and Carucci, D.J. (2002) Genome sequence and comparative analysis of the model rodent malaria parasite *Plasmodium yoelii yoelii*. *Nature* **419**, 512–519
8. Uyemura, S.A., Luo, S., Vieira, M., Moreno, S.N., and Docampo, R. (2004) Oxidative phosphorylation and rotenone-insensitive malate- and NADHquinone oxidoreductases in *Plasmodium yoelii yoelii* mitochondria *in situ*. *J. Biol. Chem.* **279**, 385–393
9. Matsushita, K., Ohnishi, T., and Kaback, H.R. (1987) NADH-ubiquinone oxidoreductases of the *Escherichia coli* aerobic respiratory chain. *Biochemistry* **26**, 7732–7737
10. Takeo, S., Kokaze, A., Ng, C.S., Mizuchi, D., Watanabe, J.I., Tanabe, K., Kojima, S., and Kita, K. (2000) Succinate dehydrogenase in *Plasmodium falciparum* mitochondria: molecular characterization of the *SDHA* and *SDHB* genes for the catalytic subunits, the flavoprotein (Fp) and iron–sulfur (Ip) subunits. *Mol. Biochem. Parasitol.* **107**, 191–205
11. Fry, M., Webb, E., and Pudney, M. (1990) Effect of mitochondrial inhibitors on adenosinetriphosphate levels in *Plasmodium falciparum*. *Comp. Biochem. Physiol. B* **96**, 775–782
12. Vaidya, A.B. and Mather, M.W.A. (2005) Post-genomic view of the mitochondrion in malaria parasites. *Curr. Top. Microbiol. Immunol.* **295**, 233–250
13. Painter, H.J., Morrisey, J.M., Mather, M.W., and Vaidya, A.B. (2007) Specific role of mitochondrial electron transport in blood-stage *Plasmodium falciparum*. *Nature* **446**, 88–91
14. Fry, M. and Pudney, M. (1992) Site of action of the antimalarial hydroxynaphthoquinone, 2-[trans-4-(4′-chlorophenyl)cyclohexyl]-3-hydroxy-1,4-naphthoquinone (566C80). *Biochem. Pharmacol.* **43**, 1545–1453
15. Biagini, G.A., Viriyavejakul, P., O'Neill, P.M., Bray, P.G., and Ward, S.A. (2006) Functional characterization and target validation of alternative Complex I of *Plasmodium falciparum* mitochondria. *Antimicrob. Agents Chemother.* **50**, 1841–1851
16. Srivastava, I.K., Rottenberg, H., and Vaidya, A.B. (1997) Atovaquone, a broad spectrum antiparasitic drug, collapses mitochondrial membrane potential in malarial parasite. *J. Biol. Chem.* **272**, 3961–3966
17. Uyemura, S.A., Luo, S., Moreno, S.N.J., and Docampo, R. (2000) Oxidative phosphorylation, Ca^{2+} transport, and fatty acid-induced uncoupling in malaria parasites mitochondria. *J. Biol. Chem.* **275**, 9709–9715
18. Daily, J.P., Scanfeld, D., Pochet, N., Roch, K.L., Plouffe, D., Kamel, M., Sarr, O., Mboup, S., Ndir, O., Wypij, D., Lavasseur, K., Thomas, E., Tamayo, P., Dong, C., Zhou, Y., Lander, E.S., Ndiaye, D., Wirth, D., Winzeler, E.A., Mesirov, J.P., and Regev, A. (2007)

Distinct physiological states of *Plasmodium falciparum* in malaria-infected patients. *Nature* **450**, 1091–1095
19. Homewood, C.A. and Neame, K.D. (1976) Comparison of methods used for removal of white cells from malaria-infected blood. *Ann. Trop. Med. Parasitol.* **70**, 249–251
20. Takashima, E., Takamiya, S., Takeo, S., Mi-ichi, F., Amino, H., and Kita, K. (2001) Isolation of mitochondria from *Plasmodium falciparum* showing dihydroorotate dependent respiration. *Parasitol. Int.* **50**, 273–278
21. Johnson, D. and Lardy, H. (1967) Isolation of liver or kidney mitochondria in *Methods Enzymol.* Vol. 10, (Estabrook, R.W. and Pullman, M.E., eds.), pp. 94–96, Academic Press, New York
22. Mogi, T., Ui, H., Shiomi, K., Ōmura, S., and Kita, K. (2008) Gramicidin S identified as a potent inhibitor for cytochrome *bd*-type quinol oxidase. *FEBS Lett.* **582**, 2299–2302
23. Wittig, I., Karas, M., and Schagger, H. (2007) High resolution clear native electrophoresis for in-gel functional assays and fluorescence studies of membrane protein complexes. *Mol. Cell Proteomics* **6**, 1215–1122
24. Kobayashi, T., Sato, S., Takamiya, S., Komaki-Yasuda, K., Yano, K., Hirata, A., Onitsuka, A., Hata, M., Mi-ichi, F., Tanaka, T., Hase, T., Miyajima, A., Kawazu, S., Watanabe, Y., and Kita, K. (2007) Mitochondria and apicoplast of *Plasmodium falciparum*: behaviour on subcellular fractionation and the implication. *Mitochondrion* **7**, 125–132
25. Mi-Ichi, F., Miyadera, H., Kobayashi, T., Takamiya, S., Waki, S., Iwata, S., Shibata, S., and Kita, K. (2005) Parasite mitochondria as a target of chemotherapy: inhibitory effect of licochalcone A on the *Plasmodium falciparum* respiratory chain. *Ann. NY Acad. Sci.* **1056**, 46–54
26. Ueno, H., Miyoshi, H., Ebisui, K., and Iwamura, H. (1994) Comparison of the inhibitory action of natural rotenone and its stereoisomers with various NADH-ubiquinone reductases. *Eur. J. Biochem.* **225**, 411–417
27. Tushurashvili, P.R., Gavrikova, E.V., Ledenev, A.N., and Vinogradov, A.D. (1985) Studies on the succinate dehydrogenating system. Isolation and properties of the mitochondrial succinate-ubiquinone reductase. *Biochim. Biophys. Acta* **809**, 145–159
28. Miyadera, H., Shiomi, K., Ui, H., Yamaguchi, Y., Masuma, R., Tomoda, H., Miyoshi, H., Osanai, A., Kita, K., and Omura, S. (2003) Atpenins, potent and specific inhibitors of mitochondrial complex II (succinate-ubiquinone oxidoreductase). *Proc. Natl Acad. Sci. USA* **100**, 473–477
29. Suraveratum, N., Krungkrai, S.R., Leangaramgul, P., Prapunwattana, P., and Krungkrai, J. (2000) Purification and characterization of *Plasmodium falciparum* succinate dehydrogenase. *Mol. Biochem. Parasitol.* **105**, 215–222
30. Yankovskaya, V., Horsefield, R., Tornroth, S., Luna-Chavez, C., Miyoshi, H., Leger, C., Byrne, B., Cecchini, G., and Iwata, S. (2003) Architecture of succinate dehydrogenase and reactive oxygen species generation. *Science* **299**, 700–704
31. Sun, F., Huo, X., Zhai, Y., Wang, A., Xu, J., Su, D., Bartlam, M., and Rao, Z. (2005) Crystal structure of mitochondrial respiratory membrane protein complex II. *Cell* **121**, 1043–1057
32. Huang, L.S., Sun, G., Cobessi, D., Wang, A.C., Shen, J.T., Tung, E.Y., Anderson, V.E., and Berry, E.A. (2006) 3-Nitropropionic acid is a suicide inhibitor of mitochondrial respiration that, upon oxidation by Complex II, forms a covalent adduct with a catalytic base arginine in the active site of the enzyme. *J. Biol. Chem.* **281**, 5965–5972
33. Schägger, H. and Pfeiffer, K. (2000) Supercomplexes in the respiratory chains of yeast and mammalian mitochondria. *EMBO J.* **19**, 1777–1783
34. Kerscher, S.J. (2000) Diversity and origin of alternative NADH:ubiquinone oxidoreductase. *Biochim. Biophys. Acta* **1459**, 274–283
35. De Vries, S. and Grivell, L.A. (1988) Purification and characterization of a rotenone-insensitive NADH:Q_6 oxidoreductase from mitochondria of *Saccharomyces cerevisiae*. *Eur. J. Biochem.* **176**, 377–341
36. Björklöf, K., Zickermann, V., and Finel, M. (2000) Purifiction of the 45 kDa, membrane bound NADH dehydrogenase of *Escherichia coli* (NDH-2) and analysis of its interaction with ubiquinone analogs. *FEBS Lett.* **467**, 105–110
37. Kerscher, S.J., Okun, J.G., and Brandt, U. (1999) A single external enzyme confers alternative NADH:ubiquinone oxidoreductase activity in *Yarrowia lipolytica*. *J. Cell Sci.* **112**, 2347–2354
38. Rasmusson, A.G., Fredlund, K.M., and Møller, I.M. (1993) Purification of a rotenone-insensitive NAD(P)H dehydrogenase from the inner surface of red beetroot mitochondria. *Biochim. Biophys. Acta* **1141**, 107–110
39. Luethy, M.H., Thelen, J.J., Knudten, A.F., and Elthon, T.E. (1995) Purification, characterization, and submitochondrial localization of a 58-kilodalton NAD(P)H dehydrogenase. *Plant Physiol.* **107**, 443–450
40. Yamashita, T., Nakamaru-Ogiso, E., Miyoshi, H., Matsuo-Yagi, A., and Yagi, T. (2007) Roles of bound quinone in the single subunit NADH-quinone oxidoreductase (Ndi1) from *Saccharomyces cerevisiae*. *J. Biol. Chem.* **282**, 6012–6020
41. Miyoshi, H., Takegami, K., Sakamoto, K., Mogi, T., and Iwamura, H. (1999) Characterization of the ubiquinol oxidation sites in cytochromes *bo* and *bd* from *Escherichia coli* using aurachin C analogues. *J. Biochem.* **125**, 138–142
42. Yano, T., Li, L.-S., Weinstein, E., The, J.-S., and Rubin, H. (2006) Steady-state kinetics and inhibitory action of antitubercular phenothiazines on *Mycobacterium tuberculosis* type-II NADH-menaquinone oxidoreductase (NDH-2). *J. Biol. Chem.* **281**, 11456–11463
43. Roos, M.H. and Tielens, A.G.M. (1994) Differential expression of two succinate dehydrogenase subunit-B genes and a transition in energy metabolism during the development of the parasitic nematode *Haemonchus contortus*. *Mol. Biochem. Parasitol.* **66**, 273–281
44. Saruta, F., Kuramochi, T., Nakamura, K., Takamiya, S., Yu, Y., Aoki, T., Sekimizu, K., Kojima, S., and Kita, K. (1995) Stage-specific isoforms of complex II (succinate-ubiquinone oxidoreductase) in mitochondria from the parasitic nematode, *Ascaris suum*. *J. Biol. Chem.* **270**, 928–932
45. Morales, J., Mogi, T., and Kita, K. (2008) Divergence in structure of mitochondrial respiratory Complex II (succinate-ubiquinone reductase) revealed by protozoan enzymes. *Biochim. Biophys. Acta* **1777**, S94–S95
46. Oyedotun, K.S. and Lemire, B.D. (1999) The *Saccharomyces cerevisiae* succinate-ubiquinone oxidoreductase. Identification of Sdh3p amino acid residues involved in ubiquinone binding. *J. Biol. Chem.* **274**, 23956–23962
47. Krungkrai, J., Kanchanarithisak, R., Krungkrai, S.R., and Sunant Rochanakij, S. (2002) Mitochondrial NADH dehydrogenase from *Plasmodium falciparum* and *Plasmodium berghei*. *Exp. Parasitol.* **100**, 54–61
48. Vaidya, A.B., Painter, H.J., Morrisey, J.M., and Mather, M.W. (2008) The validity of mitochondrial dehydrogenases as antimalarial drug targets. *Trends Parasitol.* **24**, 8–9
49. Saleh, A., Friesen, J., Baumeister, S., Gross, G., and Bohne, W. (2007) Growth inhibition of *Toxoplasma gondii* and *Plasmodium falciparum* by nanomolar concentrations of 1-hydroxy-2-dodecyl-4(1*H*)quinolone, a high-affinity inhibitor of alternative (type II) NADH dehydrogenases. *Antimicrob. Agents Chemother.* **51**, 1217–1222
50. Eschemann, A., Galkin, A., Oettmeier, W., Brandt, U., and Kerscher, S. (2005) HDQ (1-hydroxy-2-dodecyl-4(1*H*)quinolone), a high affinity inhibitor for mitochondrial

alternative NADH dehydrogenase: evidence for a ping-pong mechanism. *J. Biol. Chem.* **280**, 3138–3142
51. Speijer, D., Breek, C.K., Muijsers, A.O., Hartog, A.F., Berden, J.A., Albracht, S.P., Samyn, B., van Beeumen, J., and Benne, R. (1997) Characterization of the respiratory chain from cultured *Crithidia fasciculate*. *Mol. Biochem. Parasitol.* **85**, 171–186
52. Nelson, R.E., Aphasizheva, I., Falick, A.M., Nebohacova, M., and Simpson, L. (2004) The I-complex in *Leishmania tarentolae* is an uniquely-structured F_1-ATPase. *Mol. Biochem. Parasitol.* **135**, 221–224
53. Minagawa, N., Yabu, Y., Kita, K., Nagai, K., Ohta, N., Meguro, K., Sakajo, S., and Yoshimoto, A. (1997) An antibiotic, ascofuranone, specifically inhibits respiration and in vitro growth of long slender bloodstream forms of *Trypanosoma brucei brucei*. *Mol. Biochem. Parasitol* **84**, 271–280
54. Saimoto, H., Shigemasa, Y., Kita, K., Yabu, Y., Hosokawa, T., and Yamamoto, M. (2007) Novel phenol derivatives and antitrypanosoma preventive/therapeutic agent comprising the same as active ingredient. U.S. Patent 20070208078

Biochimica et Biophysica Acta 1787 (2009) 129–133

Contents lists available at ScienceDirect

Biochimica et Biophysica Acta

journal homepage: www.elsevier.com/locate/bbabio

Antibiotics LL-Z1272 identified as novel inhibitors discriminating bacterial and mitochondrial quinol oxidases

Tatsushi Mogi [a,*], Hideaki Ui [b], Kazuro Shiomi [b], Satoshi Ōmura [b], Hideto Miyoshi [c], Kiyoshi Kita [a]

[a] Department of Biomedical Chemistry, Graduate School of Medicine, The University of Tokyo, Hongo, Bunkyo-ku, Tokyo 113-0033, Japan
[b] Kitasato Institute for Life Sciences and Graduate School of Infection Control Sciences, Kitasato University, Shirokane, Minato-ku, Tokyo 108-8641, Japan
[c] Division of Applied Life Sciences, Graduate School of Agriculture, Kyoto University, Sakyo-ku, Kyoto 606-8502, Japan

ARTICLE INFO

Article history:
Received 9 October 2008
Received in revised form 21 November 2008
Accepted 26 November 2008
Available online 10 December 2008

Keywords:
Quinol oxidase
Inhibitor
Natural antibiotic
Escherichia coli
Trypanosoma brucei
Alternative oxidase

ABSTRACT

To counter antibiotic-resistant bacteria, we screened the Kitasato Institute for Life Sciences Chemical Library with bacterial quinol oxidase, which does not exist in the mitochondrial respiratory chain. We identified five prenylphenols, LL-Z1272β, γ, δ, ε and ζ, as new inhibitors for the *Escherichia coli* cytochrome *bd*. We found that these compounds also inhibited the *E. coli bo*-type ubiquinol oxidase and trypanosome alternative oxidase, although these three oxidases are structurally unrelated. LL-Z1272β and ε (dechlorinated derivatives) were more active against cytochrome *bd* while LL-Z1272γ, δ, and ζ (chlorinated derivatives) were potent inhibitors of cytochrome *bo* and trypanosome alternative oxidase. Thus prenylphenols are useful for the selective inhibition of quinol oxidases and for understanding the molecular mechanisms of respiratory quinol oxidases as a probe for the quinol oxidation site. Since quinol oxidases are absent from mammalian mitochondria, LL-Z1272β and δ, which are less toxic to human cells, could be used as lead compounds for development of novel chemotherapeutic agents against pathogenic bacteria and African trypanosomiasis.

1. Introduction

The emergence of antibiotic-resistant strains of major pathogenic bacteria such as *Staphylococcus aureus* is an increasingly serious public health concern [1]. To evade bacterial drug-resistance mechanisms, new effective chemotherapeutic agents, which have novel mechanisms of action as well as different cellular targets compared with conventional antibiotics, need to be developed [2].

Cytochromes *bo* (CyoABCD) and *bd* (CydAB) are two terminal quinol oxidases of the aerobic respiratory chain in *Escherichia coli* and many other bacteria [3,4 for reviews]. Although they are structurally unrelated, both generate proton-motive force through the oxidation of quinols coupled to dioxygen reduction. Cytochrome *bo* is a proton-pumping heme–copper terminal oxidases and is predominantly expressed under highly aerated growth conditions. In contrast, cytochrome *bd* is a predominant terminal oxidase under microaerophilic growth conditions and performs a variety of physiological functions such as microaerophilic respiration and protection against oxygen stress. Further, cytochrome *bd* and its variant cyanide-insensitive oxidase (CioAB) play a key role in survival and adaptation of pathogenic bacteria that encounter host environments where dioxygen is progressively limited [5–9].

In long slender bloodstream forms of the parasitic protist *Trypanosoma brucei*, which causes sleeping sickness in human and nagana in livestock, mitochondrial respiratory Complexes III and IV are down-regulated and alternative quinol oxidase (AOX) serves as a terminal oxidase [10,11]. AOX is a di-iron family protein bound to the matrix side of the inner membrane and cannot generate the proton-motive force. All three quinol oxidases have no counterparts in mammalian mitochondria, thus they are potential targets for novel antimicrobial chemotherapeutics. In fact, we previously identified ascofuranone (AF), a prenylphenol isolated from a phytopathogenic fungus *Ascochyta viciae* [12], as a potent inhibitor for the growth of *T. brucei* and trypanosome AOX (noncompetitive inhibition with IC_{50} of 2 nM) [13,14].

By screening of hundreds of natural antibiotics in the Kitasato Institute for Life Sciences Chemical Library [15] with the *E. coli* cytochrome *bd*, we found that LL-Z1272γ has potent inhibititory activity. We extended our screening to related compounds and found that antibiotics LL-Z1272β, γ, δ, ε and ζ (Fig. 1), prenylphenols isolated from the fungus *Verticillum* sp. FO-2787 [16], are a unique set of natural compounds that can discriminate and inhibit alternative respiratory quinol oxidases. Thus, antibiotics LL-Z1272 are useful probes for understanding of molecular mechanisms of quinol oxidases and we hope that our findings contribute to the development of new antibiotics.

2. Materials and methods

2.1. Isolation or source of antibiotics and inhibitors

LL-Z1272β, γ, δ, ε and ζ were isolated from the cultured mycelium *Verticillum* sp. FO-2787 [16]. Antibiotics LL-Z1272α, β, γ,

* Corresponding author. Tel.: +81 3 5841 8202; fax: +81 3 5841 3444.
E-mail address: tmogi@m.u-tokyo.ac.jp (T. Mogi).

0005-2728/$ – see front matter © 2008 Elsevier B.V. All rights reserved.
doi:10.1016/j.bbabio.2008.11.016

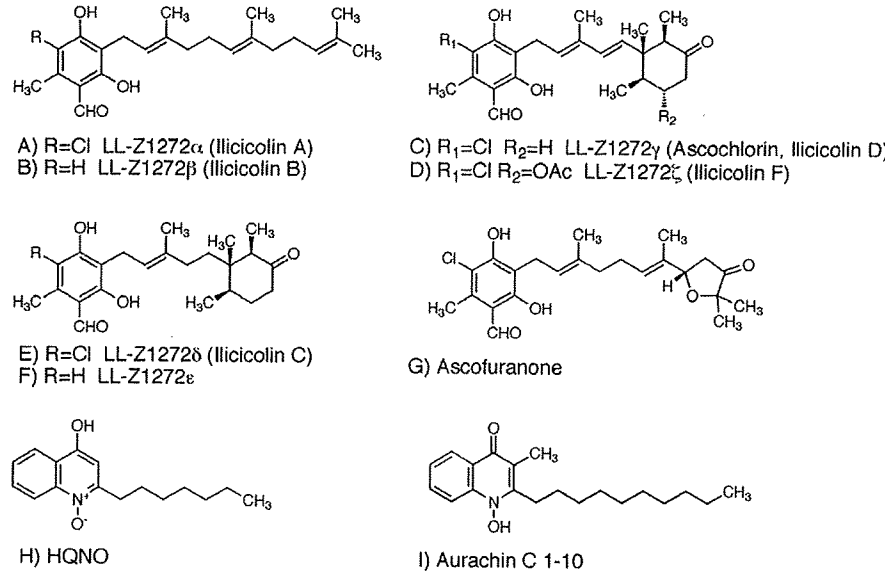

Fig. 1. Structures of antibiotics LL-Z1272 and related natural compounds.

δ, ε and ζ have been originally isolated from an imperfect fungus *Fusarium* sp. as inhibitors for the growth of the protist *Tetrahymena pyriformis* [17]. Ilicicolin A, B, D, C, and F isolated from the fungus *Cylindrocladium ilicicola* [18] are also identical to LL-Z1272α, β, γ, δ, and ζ, respectively [19]. AF and piericidin A were kind gifts from Drs. Masaichi Yamamoto (aRigen Pharmaceuticals. Inc.) and Shigeo Yoshida (Institute of Physical and Chemical Research), respectively. Synthesis of aurachin C 1-10 was described previously [20]. Antimycin A_1 and 2-heptyl-4-hydroxyquinoline *N*-oxide (HQNO) were purchased from Sigma.

2.2. Preparation of cytoplasmic membrane vesicles and purification of cytochrome bo

Cytochrome *bd*-overproduced membranes were isolated from *E. coli* ST4683/pNG2 (Δ*cyo* Δ*cyd*/*cyd*$^+$ Tet^R), which can overproduce *bd*-type quinol oxidase as the sole terminal oxidase [21]. Heme *d* content was 2.1±0.1 nmol/mg protein (*i.e.* approximately 20% of membrane proteins). Cytochrome *bo*-type quinol oxidase was purified from cytoplasmic membranes of *E. coli* GO103/pHN3795-1 (*cyo*$^+$ Δ*cyd*/*cyo*$^+$ Amp^R), as described previously [22]. Trypanosome AOX-overproduced membranes were isolated from *E. coli* FN102 (BL21 (DE3) Δ*hemA*)/pTvAOX, which can express *Trypanosoma vivax* AOX as the sole functional quinol oxidase [23]. The expression level of AOX was estimated to be ~5% of membrane proteins by SDS-polyacrylamide gel electrophoresis.

2.3. Quinol oxidase assay

The activity of the *E. coli* quinol oxidases was determined at 25 °C with a V-660 double monochromatic spectrophotometer (JASCO, Tokyo, Japan) with data acquisition at 0.05 s. The reaction mixture (1 ml) contained 50 mM potassium phosphate (pH 6.5), and 0.02% Tween 20 (protein grade, Calbiochem) [24]. Enzyme concentrations were 2.4 nM for cytochrome *bd* and 2 nM for cytochrome *bo*. Reactions were started by addition of ubiquinol-1 (Q_1H_2) at a final concentration of 100 μM, and the activity was calculated by using a molar extinction coefficient of 12,300 at 278 nm. The activity of *T. vivax* AOX was measured in 50 mM Tris–HCl (pH 7.4)–0.1% sucrose monolaurate (Mitsubishi-Kagaku Foods Co., Tokyo, Japan). Enzyme kinetics were analyzed based on the modified *ping-pong bi-bi* mechanism for cytochrome *bd* [21] or the Michaelis–Menten mechanism for cytochrome *bo* and *T. vivax* AOX, by using KaleidaGraph ver. 4.0 (Synergy Software, Reading, PA).

2.4. Dose–response analysis

Duplicate assays were performed at each concentration with two independent preparations of membranes. Dose–response data were analyzed by the nonlinear regression curve-fitting with KaleidaGraph ver. 4.0 as described previously [24]. IC_{50} values in the presence of 100 μM Q_1H_2 were estimated by using the equation for the relative residual activity; $v=1/(1+([\text{Inhibitor}]/IC_{50})^n)$ where n is the Hill coefficient [24].

3. Results

3.1. Analysis of inhibition of cytochrome bd by antibiotics LL-Z1272

In the course of our screening for inhibitors against the *E. coli* cytochrome *bd*, we identified LL-Z1272γ as an antibiotic that suppressed the Q_1H_2 oxidation by the cytochrome *bd*-overproduced membranes (84% inhibition at 5 μg/ml) greater than antimycin A (50%), a non-competitive inhibitor of cytochrome *bd* [25]. We extended our screening with antibiotics LL-Z1272β, γ, δ, ε and ζ, prenylphenols isolated from *Verticillum* sp. FO-2787 [16], and found that LL-Z1272β and ε were more potent inhibitors for cytochrome *bd*. These compounds do not have a chlorine atom at position 5 of the phenol ring (Fig. 1), and the cyclohexanone ring of LL-Z1272ε slightly increased the binding affinity to cytochrome *bd* (Table 1). The 50% inhibitory concentrations (IC_{50}) for LL-Z1272β and ε (dechlorinated derivatives) were determined to be 2.1 and 1.1 μM (average values of two independent preparations), respectively, and are one-order of magnitude smaller than those of LL-Z1272γ, δ and ζ (chlorinated derivatives) (Table 1). The IC_{50} values for known inhibitors for cytochrome *bd* [20,25–27] are 10 μM for piericidin A, 5 μM for antimycin A, 1 μM for HQNO, and 8.3 nM for aurachin C 1–10.

Table 1
Summary on IC_{50} values of quinol oxidase inhibitors for the *E. coli* cytochrome *bd* and *bo* and *T. vivax* AOX

Compounds	Cytochrome *bd*[a]	Cytochrome *bo*[b]	trypanosome AOX[c]
LL-Z1272β	2.1±0.1[d]	1.2±0.1	0.18±0.02
LL-Z1272γ	81±17	0.082±0.016	0.015±0.001
LL-Z1272δ	32±4	0.28±0.02	0.046±0.004
LL-Z1272ε	1.1±0.1	7.2±0.7	0.65±0.09
LL-Z1272ζ	85±7	0.37±0.02	0.43±0.02
Ascofuranone	47±10	0.062±0.003	0.0049±0.0002
Aurachin C 1–10	0.0083±0.0003	0.0023±0.0001	28±2

[a] The *E. coli* cytochrome *bd*-overproduced membranes.
[b] The purified *E. coli* cytochrome *bo*.
[c] The *T. vivax* AOX-overproduced membranes.
[d] μM.

3.2. Kinetic analysis of inhibition of cytochrome bd by LL-Z1272β and ε

Effects of LL-Z1272β and ε on the Q_1H_2 oxidation by cytochrome *bd* were further analyzed kinetically. Control data were analyzed based on the modified *ping-pong bi-bi* mechanism by assuming the stabilization of dioxygen reduction intermediates [28] and apparent K_m and V_{max} values for the control were determined to 50 μM and 2364 Q_1H_2/enzyme/s, respectively, in 50 mM potassium phosphate (pH 6.5)–0.02% Tween 20 [24] (Fig. 2). In the presence of inhibitors, reactions followed the Michaelis–Menten kinetics (Fig. 2). LL-Z1272β acts as a noncompetitive inhibitor with K_i=7.6±2.5 μM while LL-Z1272ε serves as a competitive inhibitor with K_i=1.00±0.03 μM (Fig. 2).

3.3. Dose–response analysis of inhibition of cytochrome bo by antibiotics LL-Z1272

In contrast to *bd*-type oxidase, the Q_1H_2 oxidase activity of the *E. coli* cytochrome *bo* was more sensitive to chlorinated derivatives, LL-Z1272γ, ε and ζ. IC_{50} values for LL-Z1272β, γ, δ, ε and ζ (averages from two preparations) were determined to be 1.2, 0.082, 0.28, 7.2 and 0.37 μM, respectively (Table 1). The IC_{50} values for known inhibitors for cytochrome *bo* [20,27,29–31] are 0.3 μM for HQNO, 0.14 μM for piericidin A, and 2.3 nM for aurachin C 1–10, showing that cytochrome *bo* is more sensitive to these quinone analogs than cytochrome *bd*. It should be noted that LL-Z1272γ is a very potent inhibitor of cytochrome *bo*.

3.4. Kinetic analysis of inhibition of cytochrome bo by antibiotics LL-Z1272

Effects of LL-Z1272β, γ, δ, and ζ on the Q_1H_2 oxidation by cytochrome *bo* were further analyzed kinetically at different concentrations of inhibitors. Enzyme kinetics were analyzed based on the Michaelis–Menten mechanism [29,31], and we found that the inhibition mechanism was all mixed-type (Fig. 3). It should be noted that due to changes in assay conditions apparent K_m and V_{max} values were shifted to 23 μM and 1035 Q_1H_2/enzyme/s, respectively (Fig. 3), from 50 μM and 515 Q_1H_2/enzyme/s, respectively, in 50 mM Tris–HCl (pH 7.4)–0.1% sucrose monolaurate in our previous study [32].

3.5. Dose–response analysis of inhibition of trypanosome AOX by antibiotics LL-Z1272

Because of the structural similarity of antibiotics LL-Z1272 with trypanocidal AF (Fig. 1), we examined the effects of antibiotics LL-Z1272 on Q_1H_2 oxidase activity of *T. vivax* AOX. From dose–response analysis with the AOX-overproduced *E. coli* membranes, we determined IC_{50} values for LL-Z1272β, γ, δ, ε, ζ, AF and aurachin C1–10 to be 180, 15, 46, 650, 430, 4.9 nM and 28 μM, respectively (Table 1). Our data indicate that 1) the furanone ring of AF is not essential for binding to trypanosome AOX, 2) the 5-chloride group on the phenol ring increases the binding affinity, and 3) aurachin C, the most potent inhibitor for bacterial quinol oxidases (IC_{50}=8.3 and 2.3 nM for the *E. coli* cytochrome *bd* and *bo*, respectively (Table 1)) [20,27], is 2 to 4 order of magnitude less active than the prenylphenols.

3.6. Kinetic analysis of inhibition of trypanosome AOX by antibiotics LL-Z1272

Effects of LL-Z1272β, γ, δ, ε and ζ and AF on enzyme kinetics by *T. vivax* AOX were examined in the presence of detergents. Q_1H_2 oxidation by *T. vivax* AOX followed the Michaelis–Menten kinetics

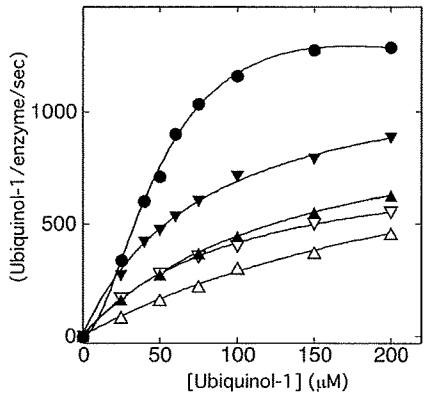

Fig. 2. Effects of antibiotics LL-Z1272 on kinetic parameters for Q_1H_2 oxidation by the *E. coli* cytochrome *bd*. Kinetic analysis was carried out in the absence of inhibitors (●) and the presence of 2 (▼) or 5 (▽) μM LL-Z1272β or 2 (▲) or 5 (△) μM LL-Z1272ε. Control data was analyzed by using the equation $v=SV_{max}/(SS(1+S/K_S)+SK_m+K_mK_m)$ where K_S indicates the constant for substrate inhibition. Data obtained in the presence of inhibitors were analyzed based on the Michaelis–Menten kinetics. The apparent K_m (μM) and V_{max} (Q_1H_2/enzyme) values obtained were 50±4 and 2364±194, respectively, for the control (K_S=381 μM), 79±5 and 1232±33, respectively, for 2 μM LL-Z1272β, 100±5 and 826±21, respectively, for 5 μM LL-Z1272β, 140±3 and 1065±12, respectively, for 2 μM LL-Z1272ε, 287±41 and 1113±107 Q_1H_2/enzyme/s, respectively, for 5 μM LL-Z1272ε, respectively.

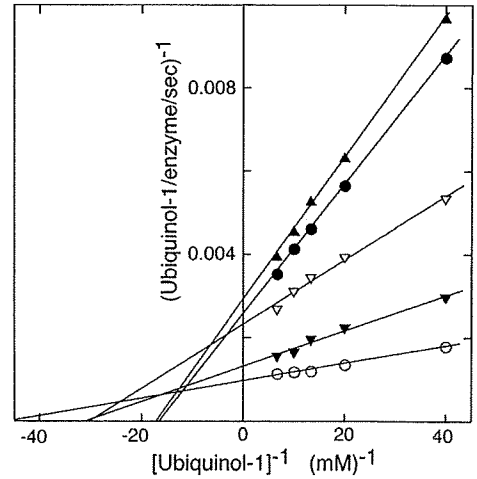

Fig. 3. Effects of antibiotics LL-Z1272 on kinetic parameters for Q_1H_2 oxidation by the *E. coli* cytochrome *bo*. Kinetic analysis was carried out in the absence of inhibitors (○) and the presence of 0.75 μM LL-Z1272β (▼), 0.2 μM LL-Z1272γ (●), 0.75 μM LL-Z1272δ (▲), and ζ (▽). Data were analyzed based on the Michaelis–Menten kinetics. The apparent K_m and V_{max} values obtained are 23±2 and 1035±28 (control), 43±4 and 841±30 (0.75 μM LL-Z1272β), 64±2 and 402±4 (0.2 μM LL-Z1272γ), 66±3 and 361±6 (0.75 μM LL-Z1272δ), 46±4 μM and 486±14 Q_1H_2/enzyme/s (0.75 μM LL-Z1272ζ), respectively. *R* values were >0.997.

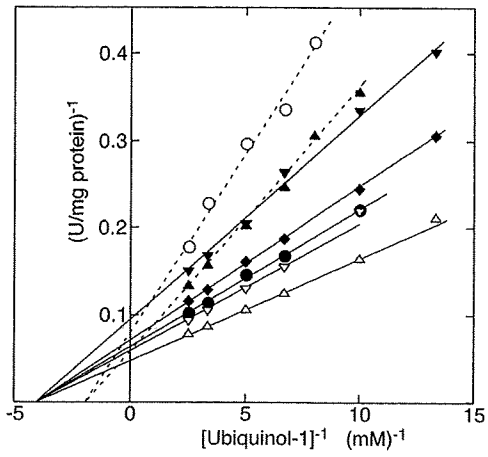

Fig. 4. Effects of antibiotics LL-Z1272 on kinetic parameters for Q_1H_2 oxidation by trypanosome AOX. Kinetic analysis was carried out in the absence of inhibitors (△) and the presence of 200 nM LL-Z1272β (▼), 20 nM LL-Z1272γ (●), 50 nM LL-Z1272δ (▲), 1 μM LL-Z1272ε (○) and 50 nM LL-Z1272ζ (▽), and 5 nM AF (♦). For clarity we showed data for one concentration of each inhibitor. The apparent K_m and V_{max} values determined for the control were 232 μM and 19.8 U/mg protein, respectively. The apparent K_i values for non-competitive inhibition by LL-Z1272β, γ, ζ, and AF were 142, 59, 203, and 2.65 nM. K_i and K_i' values for mixed-type inhibition by LL-Z1272δ and LL-Z1272ε were 0.032 and 25.5 μM and 0.483 and 9.61 μM, respectively.

and apparent K_m and V_{max} values were determined to be 232 μM and 20 U/mg protein (Fig. 4). The K_m value in 0.1% sucrose monolaurate was comparable to 350 μM for *T. b. brucei* AOX in 0.25% *n*-octyl-β-D-glucopyranoside *plus* 0.025% EDT-20 [34], but smaller than approximately 700 μM determined for *T. b. brucei* AOX in the absence of detergents [13,23]. Since the K_m value of *T. vivax* AOX for ubiquinol-2 was 116 μM (data not shown), the length of the isoprene unit may increase the binding affinity for ubiquinones [35]. The K_m of trypanosome AOX for ubiquinol-9 in *T. b. brucei* mitochondria would be comparable to the K_m value of cytochrome *bd* for ubiquinol-8 in *E. coli*.

Kinetic analysis of inhibition of *T. vivax* AOX by antibiotics LL-Z1272 revealed that LL-Z1272β (K_i=142 nM), γ (59 nM), and ζ (203 nM) act as (apparently) non-competitive inhibitors (Fig. 4), as reported for AF [13] and salicylhydroxamic acid (SHAM, K_i=25 μM) [34]. Since the amount of active AOX molecules in the *E. coli* membranes was difficult to estimate, we did not try kinetic analysis for tight-binding inhibitors [36]. In contrast, LL-Z1272δ and ε serve as mixed-type inhibitors with K_i and K_i' values of 0.032 and 25.5 μM and 0.483 and 9.61 μM, respectively.

4. Discussion

From the screening of natural antibiotics of the Kitasato Institute for Life Sciences Chemical Library, we identified prenylphenols LL-Z1272β, γ, δ, ε and ζ as a unique set of inhibitors, which can inhibit and discriminate bacterial and trypanosomal ubiquinol oxidases (Table 1). LL-Z1272β and ε (dechlorinated derivatives) inhibited cytochrome *bd*-type oxidase while LL-Z1272γ, δ, and ζ (chlorinated derivatives) were potent inhibitors of cytochrome *bo*-type oxidase and trypanosome AOX. Aurachin C is a potent inhibitor for both cytochrome *bo* and *bd* [20,27], while AF is more active against trypanosome AOX [13]. Since all three quinol oxidases are absent from mammalian mitochondria, prenylphenols could be used as lead compounds for development of novel chemotherapeutic agents [13,14,37]. However, except for the effect of LL-Z1272β on *Clostridium perfringens* (minimum inhibitory concentration of 25 μg/ml), antibiotics LL-Z1272 were ineffective against *S. aureus*, *Pseudomonas aeruginosa*, *Mycobacterium smegmatis*, and *Bacteroides fragilis*. Neither LL-Z1272γ nor LL-Z1272ε affected the aerobic growth of *E. coli* cells expressing cytochrome *bo* or *bd* as the sole terminal oxidase, likely due to the excretion by drug efflux pumps or due to the inefficient penetration through the lipopolysaccharide layer of the outer membrane.

Kinetic analysis of the inhibition of quinol oxidases by prenylphenols yielded rather complicated inhibition mechanisms (Figs. 2–4). Structural similarities of prenylphenols to ubiquinones (Fig. 1) indicate that all these compounds would act as competitive inhibitors for the quinol oxidation site. However, in many cases we found non-competitive or mixed type inhibition. In the case of tight binding inhibitors [36], Michaelis–Menten plots resemble to those of non-competitive inhibition. Alternatively, orientation of the phenol ring of prenylphenol molecules within the binding pocket will determine interactions of prenyl tails and/or the cyclohexanone ring with the protein moiety. The latter interactions would affect the former interactions. In addition, modifications of the prenyl tail (*i.e.*, the presence of the cyclohexanone or franone ring) could alter interactions with lipid bilayers and detergent micelles, which would then affect the orientation of inhibitor molecules relative to the binding pocket in quinol oxidases. Inhibition mechanisms of natural antibiotics may be inherently associated with their structural complexity, as found for inhibitors for alternative NADH dehydrogenase NDH-II [38].

Currently approved drugs for the treatment of human sleeping sickness caused by *T. b. rhodesiense* and *T. b. gambiense* are suramine, pentamidine, melarsoprol, and eflornithine [37]. They are not available for oral administration and *T. brucei* strains resistant to one or more drugs are now emerging. Thus there is an urgent need for less-toxic and more convenient new drugs against African trypanosomiasis. In parallel studies, we recently found trypanocidal activity of LL-Z1272β [39]. LL-Z1272β and LL-Z1272δ have been shown to be less toxic to human cells [18,33] and we have demonstrated that the efficacy of AF in the treatment of trypanosome-infected mice [14]. In conclusion, antibiotics LL-Z1272 are useful as probes for understanding the quinol oxidation sites of respiratory quinol oxidases and such prenylphenols are promising leading compounds for the development of new chemotherapeutic agents for African trypanosomiasis.

Acknowledgements

We thank Dr. M. Yamamoto (aRigen Pharmaceuticals, Inc., Tokyo) for AF, Dr. S. Yoshida (Institute of Physical and Chemical Research, Saitama) for piericidin A, Dr. Rokuro Masuma (Kitasato Institute for Life Sciences) for measurements of antibacterial activities of antibiotics LL-Z1272, Dr. K. Matsushita (Yamaguchi University) for his advice on enzyme assay and Dr. R. B. Gennis (University of Illinois) for the plasmid pNG2 and the *E. coli* strain GO103. This study was supported by a Grant-in-Aid for Scientific Research (20570124 to TM), Scientific Research on Priority Areas (18073004 to KK) and Creative Scientific Research (18GS0314 to KK) from the Japanese Ministry of Education, Science, Culture, Sports, and Technology.

References

[1] T.J. Foster, The *Staphylococcus aureus* "superbug", J. Clin. Invest. 114 (2004) 1693–1696.
[2] J. Travis, Reviving the antibiotic miracle? Science 264 (1994) 360–362.
[3] S. Jünneman, Cytochrome *bd* terminal oxidase, Biochim. Biophys. Acta 1321 (1997) 107–127.
[4] T. Mogi, M. Tsubaki, H. Hori, H. Miyoshi, H. Nakamura, Y. Anraku, Two terminal quinol oxidase families in *Escherichia coli*: variations on molecular machinery for dioxygen reduction, J. Biochem. Mol. Biol. Biophys. 2 (1998) 79–110.
[5] L. Cunningham, M. Pitt, H.D. Williams, The *cioAB* genes from *Pseudomonas aeruginosa* code for a novel cyanide-insensitive terminal oxidase related to the cytochrome *bd* quinol oxidases, Mol. Microbiol. 24 (1997) 579–591.
[6] S.S. Way, S. Sallustio, R.S. Magliozzo, M.B. Goldberg, Impact of either elevated or decreased levels of cytochrome *bd* expression on *Shigella flexneri* virulence, J. Bacteriol. 181 (1999) 1229–1237.

[7] S. Endley, D. McMurray, T.A. Ficht, Interruption of the *cydB* locus in *Brucella abortus* attenuates intracellular survival and virulence in the mouse model of infection, J. Bacteriol. 183 (2001) 2454–2462.
[8] A.K. Turner, L.Z. Barber, P. Wigley, S. Muhammad, M.A. Jones, M.A. Lovell, S. Hulme, P.A. Barrow, Contribution of proton-translocating proteins to the virulence of *Salmonella enterica* serovars Typhimurium, Gallinarum, and Dublin in chickens and mice, Infect. Immun. 71 (2003) 3392–3401.
[9] L. Shi, C.D. Sohaskey, B.D. Kana, S. Dawes, R.J. North, V. Mizrahi, M.L. Gennaro, Changes in energy metabolism of *Mycobacterium tuberculosis* in mouse lung and under *in vitro* conditions affecting aerobic respiration, Proc. Natl. Acad. Sci. U. S. A. 102 (2005) 15629–15634.
[10] M. Chaudhuri, R.D. Ott, G.C. Hill, Trypanosome alternative oxidase: from molecule to function, Trends Parasitol. 22 (2006) 484–491.
[11] A.L. Moore, M.S. Albury, P.G. Crichton, C. Affourtit, Function of the alternative oxidase: is it still a scavenger? Trends Plant Sci. 7 (2002) 478–481.
[12] N. Sasaki, T. Okutomi, T. Hosokawa, Y. Nawata, K. Ando, Ascofuranone, a new antibiotic from *Ascochyta viciae*, Tetrahedron Lett. 13 (1972) 2541–2544.
[13] N. Minagawa, Y. Yabu, K. Kita, K. Nagai, N. Ohta, K. Meguro, S. Sakajo, A. Yoshimoto, An antibiotic, ascofuranone, specifically inhibits respiration and in vitro growth of long slender bloodstream forms of *Trypanosoma brucei brucei*. Mol, Biochem. Parasitol. 84 (1997) 271–280.
[14] Y. Yabu, A. Yoshida, T. Suzuki, C. Nihei, K. Kawai, N. Minagawa, T. Hosokawa, K. Nagai, K. Kita, N. Ohta, The efficacy of ascofuranone in a consecutive treatment on *Trypanosoma brucei brucei* in mice, Parasitol. Int. 52 (2003) 155–164.
[15] H. Ui, A. Ishiyama, H. Sekiguchi, M. Namatame, A. Nishihara, A. Takahashi, K. Shiomi, K. Otoguro, S. Ō mura, Selective and potent *in vitro* antimalarial activities found in four microbial metabolites, J. Antibiot. 60 (2007) 220–222.
[16] S. Takamatsu, M.-C. Rho, R. Masuma, M. Hayashi, K. Komiyama, H. Tanaka, S. Omura, A novel testosterone 5a-reductase inhibitor, 8′9′-dehydroascochlorin produced by *Verticillium* sp. FO-2787, Chem. Pharm. Bull. 42 (1994) 953–956.
[17] G.A. Ellestad, R.H. Evans Jr., M.P. Kunstmann, Terpenoid metabolites from an unidentified *Fusarium* species, Tetrahedron 25 (1969) 1323–1334.
[18] S. Hayakawa, H. Minato, K. Katagiri, The ilicicolins, antibiotics from *Cylindrocladium ilicicola*, J. Antibiot. 24 (1971) 653–654.
[19] H. Minato, T. Katayama, S. Hayakawa, K. Katagiri, Identification of ilicicolins with ascochlorin and LL-Z1272, J. Antibiot. 25 (1972) 315–316.
[20] H. Miyoshi, K. Takegami, K. Sakamoto, T. Mogi, H. Iwamura, Characterization of the ubiquinol oxidation sites in cytochromes *bo* and *bd* from *Escherichia coli* using aurachin C analogues, J. Biochem. 125 (1999) 138–142.
[21] T. Mogi, S. Endo, S. Akimoto, M. Morimoto-Tadokoro, H. Miyoshi, Glutamates 99 and 107 in transmembrane helix III of subunit I of cytochrome *bd* are critical for binding of the heme b_{595}-*d* binuclear center and enzyme activity, Biochemistry 45 (2006) 15785–15792.
[22] M. Tsubaki, T. Mogi, Y. Anraku, H. Hori, Structure of heme–copper binuclear center of the cytochrome *bo* complex of *Escherichia coli*: EPR and Fourier-transform infrared spectroscopic studies, Biochemistry 32 (1993) 6065–6072.
[23] T. Suzuki, C. Nihei, Y. Yabu, T. Hashimoto, M. Suzuki, A. Yoshida, K. Nagai, T. Hosokawa, N. Minagawa, S. Suzuki, K. Kita, N. Ohta, Molecular cloning andcharacterization of *Trypanosoma vivax* alternative oxidase (AOX) gene, a target of the trypanocide ascofuranone, Parasitol. Int. 53 (2004) 235–245.
[24] T. Mogi, H. Ui, K. Shiomi, S. Ômura, K. Kita, Gramicidin S identified as a potent inhibitor for cytochrome *bd*-type quinol oxidase, FEBS Lett. 582 (2008) 2299–2302.
[25] S. Jünemann, J.M. Wrigglesworth, Antimycin inhibition of the cytochrome *bd* complex from *Azotobacter vinelandii* indicates the presence of a branched electron transfer pathway for the oxidation of ubiquinol, FEBS Lett. 345 (1994) 198–202.
[26] K. Kita, K. Konishi, Y. Anraku, Terminal oxidases of *Escherichia coli* aerobic respiratory chain. II. Purification and properties of cytochrome b_{558}-*d* complex from cells grown with limited oxygen and evidence of branched electron-carrying systems, J. Biol. Chem. 259 (1984) 3375–3381.
[27] B. Meunier, S.A. Madgwick, E. Reil, W. Ottemeier, P.R. Rich, New inhibitors of the quinol oxidation sites of bacterial cytochromes *bo* and *bd*, Biochemistry 34 (1995) 1076–1083.
[28] Y. Matsumoto, E. Muneyuki, D. Fujita, K. Sakamoto, H. Miyoshi, M. Yoshida, T. Mogi, Kinetic mechanism of quinol oxidation by cytochrome *bd* studied with ubiquinone-2 analogs, J. Biochem. 139 (2006) 779–788.
[29] K. Kita, K. Konishi, Y. Anraku, Terminal oxidases of *Escherichia coli* aerobic respiratory chain. I. Purification and properties of cytochrome b_{562}-*o* complex from cells in the early exponential phase of aerobic growth, J. Biol. Chem. 259 (1984) 3368–3374.
[30] K. Matsushita, L. Patel, H.R. Kaback, Cytochrome *o* oxidase from *Escherichia coli*. Characterization of the enzyme and mechanism of electrochemical proton gradient generation, Biochemistry 23 (1984) 4703–4714.
[31] M. Sato-Watanabe, T. Mogi, H. Miyoshi, H. Iwamura, K. Matsushita, O. Adachi, Y. Anraku, Structure–function studies on the ubiquinol oxidation site of the cytochrome *bo* complex from *Escherichia coli* using *p*-benzoquinones and substituted phenols, J. Biol. Chem. 269 (1994) 28899–28907.
[32] T. Mogi, T. Hirano, H. Nakamura, Y. Anraku, Y. Orii, Cu_B promotes both binding and reduction of dioxygen at the heme–copper binuclear center in the *Escherichia coli bo*-type ubiquinol oxidase, FEBS Lett. 370 (1995) 259–263.
[33] M. Gutiérrez, C. Theoduloz, J. Rodríguez, M. Lolas, G. Schmeda-Hirschmann, Bioactive metabolites from the fungus *Nectria galligena*, the main apple canker agent in Chile, J. Agric. Food Chem. 53 (2005) 7701–7708.
[34] R. Ott, K. Chibale, S. Anderson, A. Chipeleme, M. Chaudhuri, A. Guerrah, N. Colowick, G.C. Hill, Novel inhibitors of the trypanosome alternative oxidase inhibit *Trypanosoma brucei brucei* growth and respiration, Acta Trop. 100 (2006) 172–184.
[35] K. Sakamoto, H. Miyoshi, M. Ohshima, K. Kuwabara, K. Kano, T. Akagi, T. Mogi, H. Iwamura, Role of isoprenyl tail of ubiquinone in reaction with respiratory enzymes: studies with bovine heart mitochondrial complex I and *Escherichia coli bo*-type ubiquinol oxidase, Biochemistry 37 (1998) 15106–15113.
[36] P.R. Rich, S.A. Madgwick, D.A. Moss, The interactions of duroquinol, DBMIB and NQNO with the chloroplast cytochrome *bf* complex, Biochim. Biophys. Acta 1058 (1991) 312–328.
[37] A.H. Fairlamb, Chemotherapy of human African trypanosomiasis: current and future prospect, Trends Parasitol. 19 (2003) 488–494.
[38] T. Mogi, K. Matsushita, H. Miyoshi, H. Ui, K. Shiomi, S. Ômura, K. Kita, Identification of new inhibitors for alternative NADH dehydrogenase (NDH-II). FEMS Microbiol. Lett. (in press).
[39] K. Otoguro, A. Ishiyama, M. Namatame, A. Nishihara, T. Furusawa, R. Masuma, K. Shiomi, Y. Takahashi, H. Yamada, S. Omura, Selective and potent *in vitro* antitrypanosomal activities of ten microbial metabolites, J. Antibiot. 61 (2008) 372–378.

Glossary

AOX: alternatice quinol oxidase
HQNO: 2-heptyl-4-hydroxyquinoline *N*-oxide
IC_{50}: IC_{50}, the 50% inhibitory concentration
Q_1H_2: a reduced form of Q_1, ubiquinol-1

Cell Metabolism
Article

Fasting-Induced Hypothermia and Reduced Energy Production in Mice Lacking Acetyl-CoA Synthetase 2

Iori Sakakibara,[1,2] Takahiro Fujino,[3] Makoto Ishii,[2,4] Toshiya Tanaka,[1] Tatsuo Shimosawa,[5] Shinji Miura,[6] Wei Zhang,[7] Yuka Tokutake,[8] Joji Yamamoto,[2,9] Mutsumi Awano,[10] Satoshi Iwasaki,[1,2] Toshiyuki Motoike,[2,11] Masashi Okamura,[1,9] Takeshi Inagaki,[1] Kiyoshi Kita,[10] Osamu Ezaki,[6] Makoto Naito,[13] Tomoyuki Kuwaki,[7] Shigeru Chohnan,[8] Tokuo T. Yamamoto,[14] Robert E. Hammer,[12] Tatsuhiko Kodama,[1] Masashi Yanagisawa,[2,11] and Juro Sakai[1,2,*]
[1]Laboratory for Systems Biology and Medicine, Research Center for Advanced Science and Technology, University of Tokyo, Tokyo 153-8904, Japan
[2]ERATO, Japan Science and Technology Agency (JST), Tokyo 102-0075, Japan
[3]Department of Bioscience, Integrated Center for Sciences, Ehime University Graduate School of Medicine, Ehime 791-0295, Japan
[4]Department of Neurology, Weill Cornell Medical College of Cornell University, 525 East 68th Street, New York, NY 10021, USA
[5]Department of Clinical Laboratory, Faculty of Medicine, University of Tokyo, Tokyo 113-8655, Japan
[6]Nutritional Science Program, National Institute of Health and Nutrition, 1-23-1, Toyama, Shinjuku-ku, Tokyo 162-8636, Japan
[7]Departments of Molecular & Integrative Physiology and Autonomic Physiology, Graduate School of Medicine, Chiba University, Chiba, 260-8670, Japan
[8]Department of Bioresource Science, Ibaraki University College of Agriculture, 3-21-1 Chuo, Ami, Ibaraki 300-0393, Japan
[9]Division of Nephrology, Endocrinology, and Vascular Medicine, Department of Medicine, Tohoku University Graduate School of Medicine, Sendai 980-8574, Japan
[10]Department of Biomedical Chemistry, Graduate School of Medicine, University of Tokyo, Bunkyo-ku, Tokyo 113-0033, Japan
[11]Howard Hughes Medical Institute, Department of Molecular Genetics
[12]Department of Biochemistry
University of Texas Southwestern Medical Center, Dallas, TX 75390, USA
[13]Department of Cellular Function, Division of Cellular and Molecular Pathology, Niigata University Graduate School of Medical and Dental Sciences, Niigata 951-8510, Japan
[14]Center for Advanced Genome Research, Institute of Development, Aging, and Cancer, Tohoku University, Sendai 981-8555, Japan
*Correspondence: jmsakai-tky@umin.ac.jp
DOI 10.1016/j.cmet.2008.12.008

SUMMARY

Acetate is activated to acetyl-CoA by acetyl-CoA synthetase 2 (AceCS2), a mitochondrial enzyme. Here, we report that the activation of acetate by AceCS2 has a specific and unique role in thermogenesis during fasting. In the skeletal muscle of fasted *AceCS2*$^{-/-}$ mice, ATP levels were reduced by 50% compared to *AceCS2*$^{+/+}$ mice. Fasted *AceCS2*$^{-/-}$ mice were significantly hypothermic and had reduced exercise capacity. Furthermore, when fed a low-carbohydrate diet, 4-week-old weaned *AceCS2*$^{-/-}$ mice also exhibited hypothermia accompanied by sustained hypoglycemia that led to a 50% mortality. Therefore, AceCS2 plays a significant role in acetate oxidation needed to generate ATP and heat. Furthermore, *AceCS2*$^{-/-}$ mice exhibited increased oxygen consumption and reduced weight gain on a low-carbohydrate diet. Our findings demonstrate that activation of acetate by AceCS2 plays a pivotal role in thermogenesis, especially under low-glucose or ketogenic conditions, and is crucially required for survival.

INTRODUCTION

Mammals have evolved complex metabolic systems to survive extended periods of nutrient deprivation. Under a fed condition, mammals utilize glucose as the main metabolic fuel. Under ketogenic conditions such as fasting, low-carbohydrate diet feeding, and diabetes, fatty acids and ketone bodies are utilized as the main energy sources. Ketone bodies, utilized mainly in brain and also some in skeletal muscle and heart (Fukao et al., 2004), are produced in liver from acetyl-CoA released after β oxidation of fatty acids in mitochondria. Several lines of evidence report that acetate is synthesized in the liver and utilized as an alternative fuel under ketogenic conditions. For instance, acetate concentration in livers of starved rats is quite high (Murthy and Steiner, 1973). Also, formation of free acetate by the liver has been reported from studies utilizing isolated rat liver perfusion and studies using isolated hepatocytes (Leighton et al., 1989; Seufert et al., 1974; Yamashita et al., 2001). Acetate is generated following hydrolysis of acetyl-CoA by acetyl CoA hydrolase, an end product of fatty acid oxidation in rat liver peroxisomes (Leighton et al., 1989). However, it is not known whether acetate is actually utilized as an alternative fuel (substituting for glucose, fatty acids, or ketone bodies) in peripheral tissues such as skeletal muscle, heart, brown adipose tissues (BAT), or brain.

Acetyl-CoA synthetase (AceCS, EC 6.2.1.1) ligates acetate and CoA to generate acetyl-CoA. In mammals, there are two AceCSs with similar enzymatic properties: one, designated AceCS1, is a cytosolic enzyme, whereas AceCS2 is an enzyme of the mitochondrial matrix (Fujino et al., 2001; Luong et al., 2000). AceCS1 and AceCS2 are regulated posttranscriptionally by members of the sirtuin family of deacetylases, SIRT1 and SIRT3, respectively. Both SIRT1 and SIRT3 are upregulated during caloric restriction and have been implicated as mediating

the longevity-promoting effects of caloric restriction (Schwer and Verdin, 2008; Yang et al., 2007).

AceCS1 provides acetyl-CoA for the synthesis of fatty acids and cholesterol. AceCS1 is highly expressed in liver, and its transcription is regulated by sterol regulatory element-binding proteins (SREBPs), basic helix-loop-helix leucine zipper transcription factors that activate multiple genes involved in cholesterol and fatty acid metabolism (Ikeda et al., 2001; Luong et al., 2000). By contrast, AceCS2 produces acetyl-CoA for oxidation through the tricarboxylic acid cycle to produce ATP and CO_2 (Fujino et al., 2001). AceCS2 is highly expressed in BAT, heart, and skeletal muscle. Importantly, the levels of its mRNAs in BAT, heart, and skeletal muscle are robustly increased under ketogenic conditions, whereas the level of its mRNAs in liver was barely detectable (Fujino et al., 2001). The fasting-induced transcriptional activation of AceCS2 in the skeletal muscle is largely controlled by Krüppel-like factor 15 (KLF15), a member of the Krüppel-like family of transcription factors (Yamamoto et al., 2004) that regulates many genes involved in gluconeogenesis such as phosphoenolpyruvate carboxykinase (PEPCK) and amino acid-degrading enzymes required under ketogenic conditions (Gray et al., 2007; Teshigawara et al., 2005).

To examine whether acetate is utilized as a fuel under ketogenic conditions, we generated *AceCS2*-deficient mice. In this paper, we show that AceCS2 is essential for energy expenditure under ketogenic conditions.

RESULTS

Generation of *AceCS2*-Deficient Mice

To evaluate the role of AceCS2 in vivo, we generated mice lacking *AceCS2*. We constructed an insertion-type vector that disrupts exon 1 of the mouse *AceCS2* gene (Figure 1A). Two lines of mice harboring insertions in *AceCS2* were identified by Southern blotting (Figure 1B). Genotyping was performed by PCR (Figure 1C), and the absence of AceCS2 transcripts (Figure 1D) and protein (Figure 1E) was confirmed by quantitative real-time PCR (QRT-PCR) and immunoblot analysis, respectively. Wild-type (*AceCS2*$^{+/+}$), heterozygous (*AceCS2*$^{+/-}$), and homozygous (*AceCS2*$^{-/-}$) mice were born at frequencies predicted by simple Mendelian ratios. *AceCS2*$^{-/-}$ mice of both sexes were normally fertile and typical in appearance. No histological abnormalities were seen following light microscopy of sections obtained from multiple tissues of adult male mice, including bone, brain, stomach, heart, intestine, kidney, liver, pancreas, white adipose tissue, BAT, and skeletal muscle (data not shown). At birth, the body weight and length of *AceCS2*$^{-/-}$ mice were indistinguishable from their littermates. By the time of weaning (4 weeks of age), both male and female *AceCS2*$^{-/-}$ mice exhibited significant growth retardation (Figures S1A–S1C available online). After weaning, *AceCS2*$^{-/-}$ mice fed on normal chow diet began to catch up with *AceCS2*$^{+/+}$ mice in both body weight and body length. By 20 weeks of age, the body weight of the *AceCS2*$^{-/-}$ mice became comparable to their littermates (Figures S1A and S1B). Food intake of 4-week-old *AceCS2*$^{-/-}$ mice was slightly decreased compared to *AceCS2*$^{+/+}$ mice but became comparable to that of their littermates by 20 weeks of age (Figure S1D). Plasma parameters of *AceCS2*$^{+/+}$ and *AceCS2*$^{-/-}$ mice before weaning (2–4 weeks of age) and at 26 weeks of age are shown in Table S1. Glucose, ketone bodies, nonesterified fatty acids (NEFA), and insulin levels were indistinguishable between *AceCS2*$^{+/+}$ and *AceCS2*$^{-/-}$ mice at both 2–4 weeks of age and at 26 weeks of age (Table S1). Plasma concentration of growth hormone and

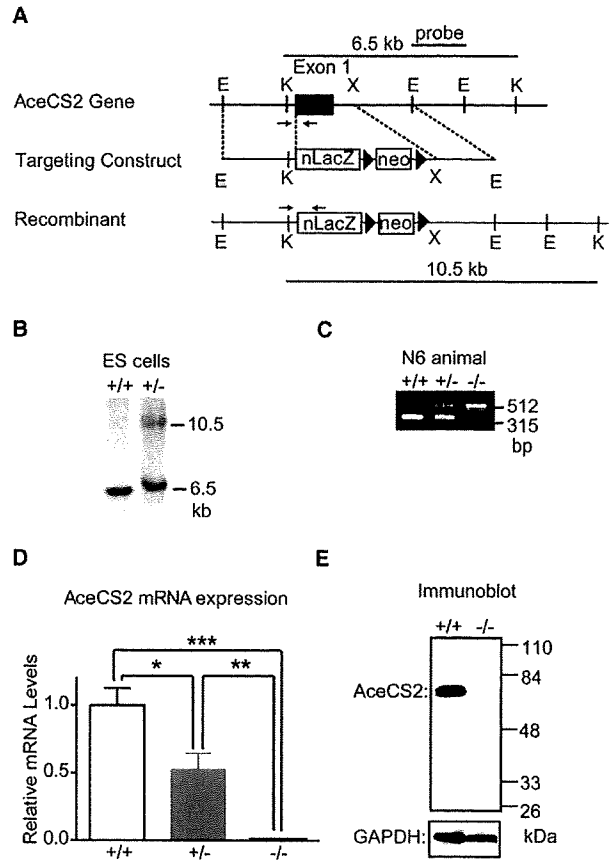

Figure 1. Generation of *AceCS2*-Deficient Mice

(A) Diagram of the targeting strategy. Only the relevant restriction sites are indicated. Locations of the probes for Southern blot analysis (bars) and PCR primers (arrows) for genotyping are shown.

(B) Southern blot analysis of KpnI-digested DNA from ES cell clones. Southern blotting was performed with the probe indicated in (A). KpnI digestion resulted in a 6.5 kb fragment in wild-type DNA and a 10.5 kb fragment in homologous recombinants.

(C) An ethidium bromide-stained agarose gel illustrates PCR products for genotyping *AceCS2*$^{+/+}$, *AceCS2*$^{+/-}$, and *AceCS2*$^{-/-}$ mice. A description of the PCR genotyping strategy is contained in the Experimental Procedures.

(D) QRT-PCR analysis of AceCS2 transcripts. Total RNA from heart of *AceCS2*$^{+/+}$, *AceCS2*$^{+/-}$, and *AceCS2*$^{-/-}$ mice were analyzed by QRT-PCR quantification as described in the Experimental Procedures. β-actin was used as the invariant control. Values represent the amount of mRNA relative to that in *AceCS2*$^{+/+}$ mice, which is arbitrarily defined as 1. Data are mean ± SEM. *$p < 0.05$ compared to *AceCS2*$^{+/+}$; **$p < 0.01$ compared to *AceCS2*$^{+/-}$; ***$p < 0.001$ compared to *AceCS2*$^{+/+}$ ($^{+/+}$, n = 9; $^{+/-}$, n = 17; $^{-/-}$, n = 7).

(E) Immunoblot analysis, with an affinity-purified anti-rabbit polyclonal AceCS2 antibody, of *AceCS2*$^{+/+}$ and *AceCS2*$^{-/-}$ mouse heart protein. Each lane was loaded with 20 μg of whole-cell lysates in SDS lysis buffer from the hearts. GAPDH was detected with a polyclonal anti-GAPDH antibody as a loading control.

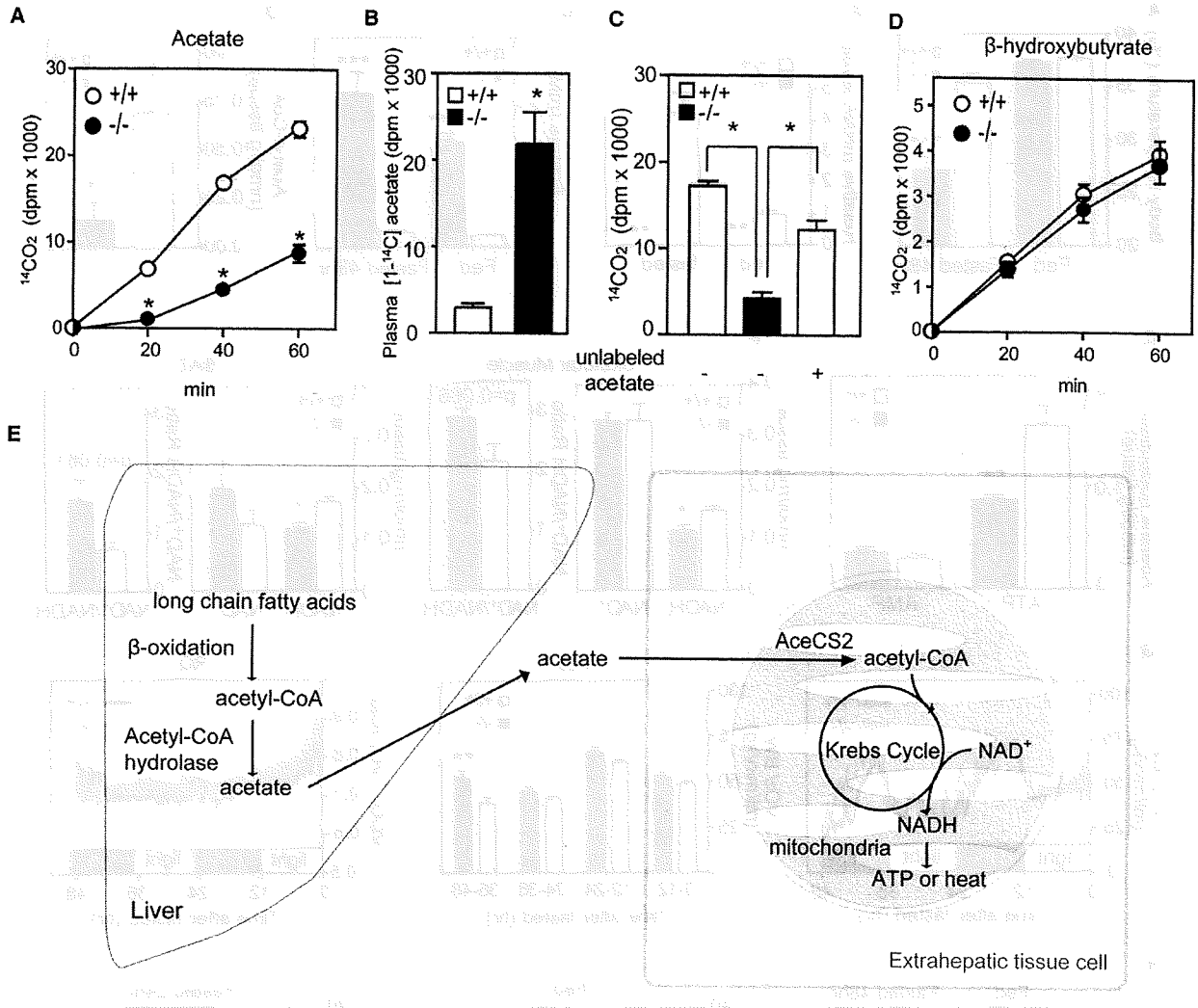

Figure 2. *AceCS2*$^{-/-}$ Mice Exhibit Lower Whole-Body Acetic Acid Oxidation during Fasting

After 48 hr of fasting, 12-week-old male mice were tested for their ability to oxidize [1-^{14}C]acetate or [1-^{14}C]β-hydroxybutyrate to $^{14}CO_2$ at 20, 40, and 60 min after intraperitoneal (i.p.) injection with the labeled compound.

(A) Rate of $^{14}CO_2$ production from acetate. *$p < 0.001$ compared to *AceCS2*$^{+/+}$.

(B) Total plasma [1-^{14}C]acetate was measured after 60 min.

(C) Rate of $^{14}CO_2$ production from acetate with inclusion of unlabeled acetate. Unlabeled acetate (0.6 g/kg) was injected with [1-^{14}C]acetate, and the acetate oxidation rate was measured after 40 min.

(D) Rate of $^{14}CO_2$ production from β-hydroxybutyrate (*AceCS2*$^{+/+}$, n = 6; *AceCS2*$^{-/-}$, n = 6).

(E) Model for the role of AceCS2 in energy metabolism.

(A–D) Data are mean ± SEM.

insulin-like growth factor-1 (IGF-1) of *AceCS2*$^{-/-}$ mice (2–4 weeks of age) were also comparable to *AceCS2*$^{+/+}$. The plasma leptin levels of 2- to 4-week-old *AceCS2*$^{-/-}$ mice were lower than those of age-matched, wild-type littermates. Notably, plasma acetate levels were markedly elevated in *AceCS2*$^{-/-}$ mice compared to *AceCS2*$^{+/+}$ mice (Table S1).

AceCS2$^{-/-}$ Mice Exhibited Marked Reduction in Whole-Body Acetate Oxidation

To examine whether acetate is, in fact, utilized as a fuel during fasting, we performed whole-body acetate oxidization assays. Mice were fasted for 48 hr and then injected with [^{14}C]acetate. Figure 2A shows the sharply decreased rate of acetate oxidation in *AceCS2*$^{-/-}$ mice. As a consequence, [^{14}C]acetate levels remained high in the plasma of *AceCS2*$^{-/-}$ mice, whereas *AceCS2*$^{+/+}$ mice showed very low levels of plasma [^{14}C]acetate (Figure 2B). Because higher levels of plasma acetate in *AceCS2*$^{-/-}$ mice might affect the acetate oxidation rate, we also examined the oxidation of [^{14}C]acetate with the inclusion of unlabeled acetate at similar levels to those found in the *AceCS2*$^{-/-}$ mice (about 2 mM) (Figure 2C). Injection of unlabeled acetate (0.6 mg/kg) led to rapid increase in plasma acetate to

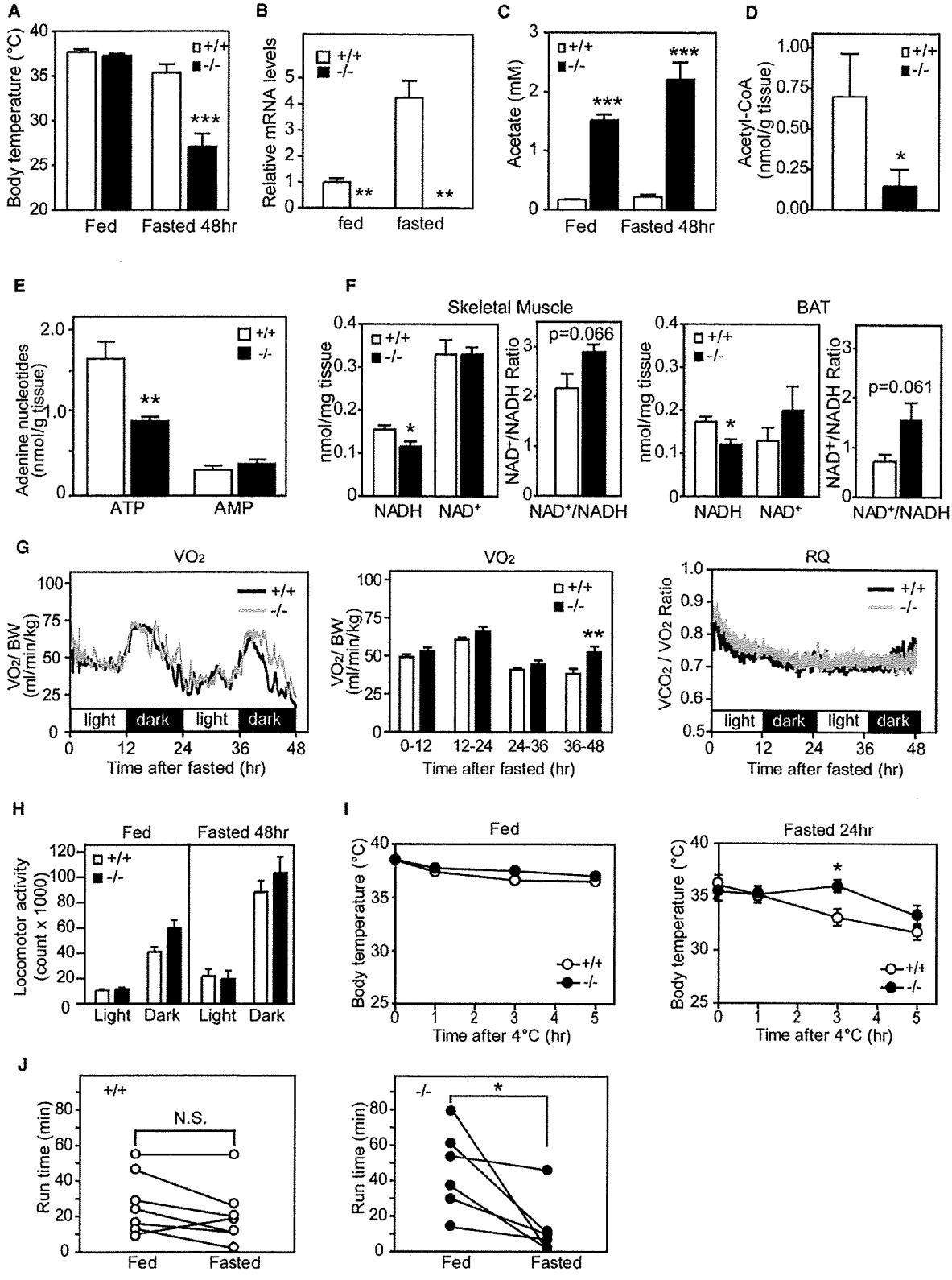
A
Body temperature (°C)
+/+
-/-
***
Fed
Fasted 48hr
B
Relative mRNA levels
**
**
fed
fasted
C
Acetate (mM)
***
***
Fed
Fasted 48hr
D
Acetyl-CoA (nmol/g tissue)
*
E
Adenine nucleotides (nmol/g tissue)
**
ATP
AMP
F
Skeletal Muscle
BAT
nmol/mg tissue
NADH
NAD+
NAD+/NADH Ratio
p=0.066
p=0.061
NAD+/NADH
G
VO2
VO2/ BW (ml/min/kg)
light
dark
Time after fasted (hr)
RQ
VCO2 / VO2 Ratio
0-12
12-24
24-36
36-48
H
Fed
Fasted 48hr
Locomotor activity (count x 1000)
Light
Dark
I
Fed
Fasted 24hr
Body temperature (°C)
Time after 4°C (hr)
J
+/+
-/-
N.S.
Run time (min)
Fed
Fasted

2 mM at 40 min after the injection (data not shown). Under this condition, the rate of acetate oxidation measured was still significantly lower in *AceCS2*$^{-/-}$ mice (Figure 2C). Oxidation of ketone bodies was similar, irrespective of genotype (Figure 2D), indicating that ketone body utilization is normal in *AceCS2*$^{-/-}$ mice.

Together with our previous report showing that [^{14}C]acetate is incorporated into CO_2 in AceCS2-transfected cells (Fujino et al., 2001), these data indicate that, in mice, acetate oxidation to form CO_2 and ATP requires AceCS2. Previous studies showed that an appreciable amount of acetate is generated in liver by hepatic acetyl-CoA hydrolase, a ubiquitous peroxisome enzyme, and that this acetate can subsequently be utilized by extrahepatic tissues (Leighton et al., 1989; Murthy and Steiner, 1973; Seufert et al., 1974). We propose a model in which acetate is generated in liver from fatty acids and released into the circulation under conditions when glucose is low, such as 48 hr fasting or low-carbohydrate/ high-fat diet. AceCS2 is necessary for salvaging this acetate for use in extrahepatic tissues such as skeletal muscle and BAT, where acetate is reactivated for reentry to the mitochondrial TCA cycle to generate ATP and heat (Figure 2E).

Adult *AceCS2*$^{-/-}$ Mice Exhibit Low Body Temperature and Reduced Capacity to Sustain Running Exercise under a Fasting Condition

To further evaluate the physiological role of acetate oxidation, 12-week-old *AceCS2*$^{-/-}$ mice were freely fed a standard rodent diet or fasted for 48 hr. During normal fed states, there was no significant difference in core temperature between *AceCS2*$^{+/+}$ and *AceCS2*$^{-/-}$ mice (Figure 3A). After 48 hr of fasting, *AceCS2*$^{+/+}$ mice were able to maintain their core body temperatures, but *AceCS2*$^{-/-}$ mice had significantly lower core body temperatures (Figure 3A). These data demonstrate that acetate activation by AceCS2 is important for maintenance of normal body temperature, likely as a result of heat production during fasting. Indeed, the mRNA levels in BAT of AceCS2 were 4-fold higher under the fasted condition than under the fed condition, suggesting that AceCS2 has an important role during fasting condition (Figure 3B).

In mice, BAT and skeletal muscle are the main thermogenic tissues in which oxidation of fatty acid, stimulated by the sympathetic nervous system, generates heat through uncoupling proteins (UCPs) present in mitochondria (Spiegelman and Flier, 2001). During fasting, the quantity and morphology of mitochondria in BAT and skeletal muscle are indistinguishable between *AceCS2*$^{+/+}$ mice and sex- and age-matched *AceCS2*$^{-/-}$ mice (Figure S2A). Oxidative proteins such as UCPs are thought to be important in thermogenesis (Matthias et al., 2000; Spiegelman and Flier, 2001). The mRNA levels of UCP1 in the BAT or UCP2 and UCP3 in the skeletal muscle did not differ significantly between *AceCS2*$^{+/+}$ and *AceCS2*$^{-/-}$ mice. Other thermogenic molecules PGC1α and PPARδ also did not differ in mRNA levels (Figure S2B and data not shown).

To evaluate substrate supply, we determined the levels of various metabolites in the plasma of fed and 48 hr fasted 12-week-old male *AceCS2*$^{+/+}$ and *AceCS2*$^{-/-}$ mice (Table S2). There was no significant change in plasma glucose or in NEFA and ketone body levels between *AceCS2*$^{+/+}$ and *AceCS2*$^{-/-}$ mice (Table S2). There was also no significant difference in the percentage of fat mass between fed *AceCS2*$^{-/-}$ and *AceCS2*$^{+/+}$ mice as assessed by dual-energy X-ray absorption (DEXA) (Table S2). However, plasma acetate was 5- to 10-fold higher in *AceCS2*$^{-/-}$ mice as compared to *AceCS2*$^{+/+}$ mice under both fed and fasted conditions (Figure 3C). These data indicate that acetate utilization is impaired in *AceCS2*$^{-/-}$ mice, implying that a deficit in extrahepatic acetate utilization causes fasting-induced hypothermia. Acetyl-CoA levels were decreased by 75% in fasted *AceCS2*$^{-/-}$ mice (Figure 3D). NADH and ATP levels in skeletal muscles of fasted *AceCS2*$^{-/-}$ mice were significantly reduced compared to those found in *AceCS2*$^{+/+}$ mice (Figures 3E and 3F). These data indicate that AceCS2 plays a pivotal role in supplying acetyl-CoA for ATP production during 48 hr of fasting. Oxygen consumption was significantly increased after 36 hr fasting, and locomotor activity was not reduced (Figures 3G and 3H).

The hypothermia in *AceCS2*$^{-/-}$ mice also differs from adaptive hypothermia in response to cold (Lowell and Spiegelman, 2000). Exposure of these *AceCS2*$^{-/-}$ mice to low temperature (4°C) did

Figure 3. *AceCS2*-Deficient Mice Exhibit Low Body Temperature and Reduced Exercise Capacity during Fasting

(A) Core temperature of male mice (12 weeks old) fed on normal chow diet was monitored after 48 hr fasting (*AceCS2*$^{+/+}$, n = 8; *AceCS2*$^{-/-}$, n = 7). *p < 0.05 compared to *AceCS2*$^{+/+}$.

(B) Relative mRNA expression levels of AceCS2 in BAT of male mice (12 weeks old, six to seven per genotype). **p < 0.01 compared to *AceCS2*$^{+/+}$.

(C) Plasma acetate levels of male mice (12 weeks old) fed or fasted for 48 hr (fed *AceCS2*$^{+/+}$, n = 4; fasted *AceCS2*$^{+/+}$, n = 4; fed *AceCS2*$^{-/-}$, n = 4; fasted *AceCS2*$^{-/-}$, n = 4).

(D) Acetyl-CoA levels in gastrocnemius muscle from 48 hr fasted male *AceCS2*$^{+/+}$ and *AceCS2*$^{-/-}$ mice (12 weeks old) were measured (*AceCS2*$^{+/+}$, n = 7; *AceCS2*$^{-/-}$, n = 8).

(E) ATP content is markedly reduced in *AceCS2*$^{-/-}$ mice. ATP and AMP contents of gastrocnemius muscle from male *AceCS2*$^{+/+}$ and *AceCS2*$^{-/-}$ mice were measured at 12 weeks of age (*AceCS2*$^{+/+}$, n = 7; *AceCS2*$^{-/-}$, n = 8). **p < 0.01 compared to *AceCS2*$^{+/+}$.

(F) NAD^+ and NADH levels and NAD^+/NADH ratio in gastrocnemius muscle and BAT of 48 hr fasted male *AceCS2*$^{+/+}$ and *AceCS2*$^{-/-}$ mice (12 weeks old) (*AceCS2*$^{+/+}$, n = 4; *AceCS2*$^{-/-}$, n = 4).

(G) Oxygen consumption (VO_2) (left panel), average of VO_2 (center panel), and RQ (respiratory quotient) (right panel) were determined in fasted male mice (12 weeks old) by indirect calorimetry (*AceCS2*$^{+/+}$, n = 6; *AceCS2*$^{-/-}$, n = 5).

(H) Total locomotor activity of male mice (14 weeks old) was measured by beam breaks in the light and dark periods (*AceCS2*$^{+/+}$, n = 12; *AceCS2*$^{-/-}$, n = 12).

(I) Male mice (12 weeks old) given food and water ad libitum were subjected to cold (4°C) (left panel) (*AceCS2*$^{+/+}$, n = 10; *AceCS2*$^{-/-}$, n = 11). Male mice (12 weeks old) fasted for 24 hr and given water ad libitum were subjected to cold (4°C) (right panel) (*AceCS2*$^{+/+}$, n = 7; *AceCS2*$^{-/-}$, n = 8). Core temperature was monitored over a 5 hr period.

(J) Male mice (12 weeks old, nine per genotype) were subjected to a run-to-exhaustion protocol on a motorized treadmill under fed conditions and 48 hr fasted conditions (*AceCS2*$^{+/+}$, n = 9; *AceCS2*$^{-/-}$, n = 9). *p < 0.05 compared to fed.

All values are mean ± SEM.